Review

Emayaruba G. Barathi Dassan, Aslina Anjang Ab Rahman*, Mohd Shukur Zainol Abidin, and Hazizan Md Akil

Carbon nanotube–reinforced polymer composite for electromagnetic interference application: A review

https://doi.org/10.1515/ntrev-2020-0064
received March 19, 2020; accepted July 21, 2020

Abstract: The growth of the application of electronic devices has created a new form of pollution known as noise or radio frequency interference, electromagnetic radiation, or electromagnetic interference (EMI), which results in the malfunction of equipment. A new carbon-based polymer composite has been unlocked through the discovery of polymer composites. Carbon nanotubes (CNTs) have shown potential as reinforcement fillers in polymer to enhance an EMI shielding material owing to their large specific surface area, well-defined 3D networking structure, and unique electronic structure. The main focus of this review is the role of CNT as fillers in intrinsic conducting polymer and conducting polymer composite. The factors that influence EMI shielding performance are also included in this review. The roles of the size; shape; and electronic, mechanical, and chemical properties of nanomaterials in tuning the EMI shielding effectiveness of polymer hybrid are emphasized. The structural design of CNT polymer composite has been reviewed as well. Future research direction has been proposed to overcome the current technological limitations and realize the most advanced EMI shielding materials for future use. The composites have a potential to replace traditional shielding materials owing to their advantageous properties.

Keywords: carbon nanotube, electromagnetic shielding materials, electromagnetic characterization, lightweight materials

* **Corresponding author: Aslina Anjang Ab Rahman,** School of Aerospace Engineering, Universiti Sains Malaysia, 14300, Penang, Malaysia, e-mail: aeaslina@usm.my
Emayaruba G. Barathi Dassan, Mohd Shukur Zainol Abidin: School of Aerospace Engineering, Universiti Sains Malaysia, 14300, Penang, Malaysia
Hazizan Md Akil: School of Materials and Mineral Resources Engineering, Universiti Sains Malaysia, 14300, Penang, Malaysia

1 Introduction

Electromagnetic interference (EMI) occurs when unwanted radiated signals or electromagnetic (EM) waves that originate from outside (ground-based transmitters) or inside (personal electronic devices) an emitter are unintentionally transmitted to another element by radiation/conduction. EMI can degrade the performance of a system or an equipment [1]. Natural phenomena, such as thunder and solar flares, and self-regulating phenomena, such as electrostatic discharge (ESD), contribute to EMI as they radiate EM waves as signals and transfer EM waves to the circuit elements of the device. Electronic devices loaded with highly integrated circuits generate undesirable EM radiations. Sensors, power transmission line, batteries, communication units, the payload of rockets, remote sensing instruments, televisions, mobile phones, computers, transformers, military and commercial planes, medical devices, space systems, and the externally located units of spacecrafts are disturbed by undesirable EMI [2]. Effective shielding materials eliminate the effect of these unwanted EM radiations. Electronic devices require lightweight and flexible materials with high-performance EMI shielding efficiency (SE) without restricting their regular flexible functionalities.

In the past, metallic and magnetic materials, such as copper, aluminum, steel, and iron, have been employed as effective shielding materials because of their high electrical conductivity and good permeability. However, despite their good EMI SE, EM pollution has not been completely eliminated or mitigated as EM signals are almost entirely reflected at the surface of the metal, which protects the environment only beyond the shield. In addition, these materials are disadvantageous in terms of weight and flexibility as today's electronic devices have become faster, smaller, and lighter [3]. Remarkable research studies have been performed on the development of polymeric materials because of their ability to shield EM waves through dominant absorption shielding, which is preferable in military

applications, such as stealth technology and camouflage. Moreover, these materials are advantageous because of their flexibility, easy processability, chemical resistance, and light weight [4,5]. Intrinsic conducting polymers (ICPs), such as polyaniline (PANI) and polypyrole (PPy), are the common choice because of their high electrical conductivity, which could be improved through chemical doping. The scope of polymer-based EMI shielding has been expanded far beyond ICP to be incorporated with insulating polymer or conducting polymer. Polymer hybrids must have high electrical conductivity/permeability to be utilized as an effective reflection/absorption shield. This property could be gained by incorporating electrically conducting/magnetic fillers into the polymer matrix. Carbon nanotubes (CNTs) have been used as conducting filler materials because these electrically conducting organic nanomaterials and their composite exhibit good EMI shielding performance. Besides, the mechanical properties of a composite can be enhanced by modifying its surface with CNT. The tensile strength and the modulus of 0.5 wt% functionalized CNT-incorporated carbon fibers (CFs) increase to about 46% (4.1 GPa) and 37% (302 GPa), respectively, compared with those of pure CFs (2.8 and 220 GPa, respectively) [6].

The high conductivity of a filler is not the only criterion needed to achieve a high-reflection type EMI shielding polymer hybrid. The principal requirement is achieving a percolated threshold network with the low filler content. A thicker interphase produces a lower percolation threshold φ_C and a smaller interphase resistance in the composites; therefore, it increases the conductivity based on the Kovacs model. In addition, short tunneling distance and poor tunneling resistivity decrease tunneling resistance and lead to more desirable conditions for electron transfer between adjacent fillers, which then improve the conductivity in composites [7]. Most of the previous studies have reported that the dispersibility of a filler within a polymer matrix is increased through the surface modification of the filler and the functionalization of the polymer to obtain a low φ_C. The alignment of fillers is crucial for enhancing electrical conductivity as it provides a path for electron transfer along the length of the composite. The electrical conductivity of poly(biphenyl dianhydride-*p*-phenylenediamine) (BPDA/PDA) polyimide (PI) reaches 183 S/cm, which is 10^{18} times higher than that of pure BPDA/PDA PI (10 S/cm) by adding highly aligned CNT [8]. The structural arrangement of conducting fillers in the composite is also very important aside from the filler content. Various structured composites, including foam/sponge, sandwiched, layered, lamellar, and segregated structures, have emphasized the importance of the structural arrangement on EMI SE. A foam/sponge/aerogel structure gives a high chance of EMI absorption because of multiple internal reflection (MIR), and the high porosity makes the material lightweight. In particular, lightweight and highly efficient EMI shielding materials are going to be the main requirements for next-generation electronic and communication devices to safeguard their smooth and continuous operation without interference from unwanted signals. Highly efficient EMI shielding with high absorption power will be preferred for advanced stealth technology in military and fighter jets.

Therefore, a comprehensive review of polymer-based EMI shielding is necessary to judge the current status and determine the possible research directions to overcome the existing drawbacks and limitations. Despite its technological importance, a detailed review on CNT–polymer nanohybrid-based EMI shielding has not been conducted to date. Thus, considering the broadness of this field, we are presenting a comprehensive review of all kinds of polymers (conducting and insulating) reinforced with the CNT filler to reflect the current state of this field. A clear future research direction is proposed to overcome existing problems and realize the most advanced EMI shielding materials for the future use. This review summarizes the current progress of polymer-based EMI shielding materials with emphasis on tunable material properties for effective shielding. The key concept of EMI shielding and its influence on material properties have been discussed in the earlier section of this review. Afterward, polymer-based materials with CNT filler and the role of individual components in the polymeric hybrid are discussed in relation to EMI SE. Finally, future research directions are proposed to realize highly efficient polymer-based EMI shielding materials with optimized physical properties.

Possible polymer and polymer composite materials with their EMI SE have been summarized. Based on Table 1, EMI SE depends on the properties of the polymer matrix and the percentage of the filler. Thicker samples generally give higher EMI SE; however, current demands are on thinner materials with high EMI SE [9].

2 EMI shielding: an overview

EMI is the intervention or disturbance of an EM signal produced or received by another electronic device. Interference can either be radiated or conducted depending on the source and transmission path.

Table 1: Electromagnetic shielding of CNT composites

Year	Polymer matrix	CNT content	Electrical conductivity, σ (S/m)	Thickness, t (mm)	EMI SE (dB)	Frequency (GHz)	Ref.
2008	PANI	25 wt% CNT	0.197	2	39.2	12–18	[4]
2017	GTR	5 wt% CNT	109.3	2.6	66.9	8–12	[10]
2011	PC	5 wt% MWCNT	—	1.85	25	8–12	[11]
2015	PVDF/ABS	1 wt% MWCNT	0.01	2	26	8–18	[12]
2013	PU	10 wt% CNT	50	2	22	8–12	[13]
2010	PP	2 wt% MWCNT	0.6	1	30–45	0.4–40	[14]
			1.4				
2018	PMMA	3 wt% MWCNT	1	3	12	8–18	[15]
			2		27		
2018	ABS	6 wt% MWCNT	0.01	2	25	8–12	[16]
2012	HDPE	1 wt% MWCNT	0.0102	0.35	16	8–12	[17]
2017	Epoxy	5 wt% MWCNT	—	1.5	25	0.3–1	[18]
2011	EVA	10 phr MWCNT	—	—	4	8–12	[19]
					6		
2015	ABS	10 wt% MWCNT	0.001	—	39	12–18	[20]
2019	PP	1.75 vol% CNT	100	3	50–74.3	8–12	[21]
2015	PVDF	4 wt% unfunctionalized MWCNT	1	0.3	110	1–18	[22]
		0.5 wt% functionalized MWCNT			98		
2016	PP/PE	5 vol% CNT	—	1	27	8–12	[23]
2009	PE	15 wt% MWCNT	315	—	13.32	0.05–1.5	[24]
	PPS		176		17.50		
2016	PS	1 wt% pristine MWCNT	0.0001	1	3	8–12	[25]
		1 wt% functionalized MWCNT	0.1		7		
2018	PC/EMA	7.5 phr MWCNT	19.1	—	34	8–12	[26]
2012	ABS	15 wt% MWCNT	520	1.1	39	0.1–1.5	[27]
2012	EMA	12.5 wt% MWCNT	0.1	5	25	8–12	[28]
2011	PMMA	2 wt% CNT	6	1	50 (solid)	0.04–40	[29]
					25 (foam)		
			0.5		—		
			1.5				
2006	PC	7 wt% MWCNT	10	—	15.95	0.05–1.5	[30]
2011	PS	5 wt% MWCNT	7.1	2	17.2	8–12	[31]
2011	PTT	4.76 vol% MWCNT	4.5	2	22	8–12	[32]
2008	EVA	15 wt% SWCNT	0.1	3.5	23	0.2–2	[33]
					29	8–12	
2010	PLLA	4 wt% MWCNT	10	0.4	16	0.036–50	[34]
2017	PC	3.5 wt% MWCNT	0.01	3.5	14	8–12	[35]
					16		
			1,000		31.41		
2016	PC	4 wt% MWCNT	—	5.6	21.6	8–12	[36]
2014	PC	5 wt% MWCNT	10	—	16	8–12	[37]
2008	PS	10 vol% MWCNT	90.3	0.2–0.3	17	8–12	[38]
	PMMA		137		18		
2011	SMP	9 wt% MWCNT	35	0.5	14	4–7	[39]
				2	35	13–16	
2019	PDMS SGM	3 vol% MWCNT	50	2.7	52–55	8–12	[40]
	HGM		45		45–47		
2013	Epoxy	20 wt% MWCNT	900	1.75	60	8–12	[41]
2014	Epoxy	10 wt% MWCNT	—	3	56.92	3.22–40	[42]
2016	PMMA	1 wt% MWCNT	—	3	0.35	0.1–1.5	[43]
2014	PC	20 wt% MWCNT	1,000	2	43	8–12	[44]
2011	Epoxy	0.5 wt% MWCNT	—	—	4.36	8–12	[45]

Table 1: Continued

Year	Polymer matrix	CNT content	Electrical conductivity, σ (S/m)	Thickness, t (mm)	EMI SE (dB)	Frequency (GHz)	Ref.
					33.38	26–37	
					14.80	78–118	
		0.5 wt% SWCNT	—	—	6.02	8–12	
					33.52	26–37	
					8.87	78–118	
2011	PVDF	7 wt% functionalized MWCNT	0.1	—	18	8–12	[46]
2013	PVDF	0.25 wt% functionalized CNT	—	0.025	37	6–12	[47]
2013	ABS	15 wt% CNT	100	1.1	50	8–12	[48]
2012	PANI/PS	7 vol% MWCNT	3.3	—	23.3	8–12	[49]
2016	PVA	2 wt% MWCNT	240	0.5	30.74	0.0003–3	[50]
			0.00014		1.95		
2018	PMMA	8 wt% MWCNT	—	2.5	36	8–12	[51]
2013	PP	10 wt% CNT	—	—	19	0.03–1.5	[52]
2018	PS	10 wt% MWCNT	100	—	22	8–12	[53]
2016	PVC	4 wt% MWCNT	—	5.6	22.6	8–12	[54]
2015	PMMA	7.3 wt% CNT	0.01	0.57	29	75–110	[55]
2010	RET	3.2 vol% functionalized SWCNT	0.1	2	25	8–12	[56]
		3.7 vol% functionalized MWCNT	—		3		
2014	PES	5 wt% MWCNT	—	5	47.5	8–12	[57]
	PEI				45.5		
2016	PDMS	2 wt% CNT	3,900	1.6	80	8–12	[58]
2018	PLA	3 wt% MWCNT	6.4	2	31.02	8–12	[59]
2015	UHMWPE	10 wt% MWCNT	—	1	50	8–12	[60]
2016	Epoxy	2 wt% CNT	516 (sponge)	2	40	8–12	[61]
		20 wt% CNT	100 (solid)		30		
2017	PLA	40 wt% CNT	17,000	0.4	55 (solid)	8–12	[9]
					30 (scaffold)		
2017	PLA	1.48 vol% CNT	2.75	3.7	21.6 (foam)	8–12	[62]
			—		17.3 (solid)		
2013	PP	5 wt% MWCNT	—	2.9	15–20	0.001–3	[63]
2011	PU	25 wt% MWCNT	10	0.1	20	8–12	[64]
2013	PU	10 wt% MWCNT	12.4	>0.2	29	8–12	[65]
2007	PU	25 wt% SWCNT	100	2	22	8–12	[66]
2013	PU	10 wt% MWCNT	790	2.5	41.6	8–12	[67]
2015	PU/PEDOT	30 wt% MWCNT	275	2.5	45	12.4–18	[68]
2004	PMMA	40 wt% MWCNT	3,000	0.06–0.165	27	0.05–13.5	[69,70]
2006	Epoxy	15 wt% SWCNT	15	1.5	30	8–12	[71]
2013	PC	15 wt% MWCNT	5.2	6	28	8–12	[72]
2011	PTT	10 wt% SWCNT	30	1.5–2	36–42	12.4–18	[73]
2015	UHMWPE	10 wt%	100	1	50	8–12	[74]
2015	PEDOT	15 wt%	1,935	2.8	58	12–18	[74]
2008	PCL	0.25 vol% MWNT	2.5	2	80	8–12	[75]
2009	PP	7.5 vol% MWCNT	—	1	36	8–12.4	[76]
2005	PS	7.0 wt% CNT	10	—	18.56	8–12	[77]
			—				
2011	PPy/EVA	18–75 phr MWCNT	—	—	45–55	0.03–1.5	[78]
2013	PDMS	5.7 vol% MWNT	100	2	80	1–12.5	[5]
2007	Epoxy	15 wt% short SWCNT	4	2	18	8–12	[79]
		15 wt% long SWCNT	20		30		
		15 wt% annealed SWCNT	15		24		

Table 1: Continued

Year	Polymer matrix	CNT content	Electrical conductivity, σ (S/m)	Thickness, t (mm)	EMI SE (dB)	Frequency (GHz)	Ref.
2008	PC	5.4 wt% SWCNT	—	3	47	1	[80]
2019	PDMS	6 wt% CNT + 40 wt% micro silica	>100	2	45	8–12	[81]
2019	PVDF	2.0 wt% CNT	5.89	1.1	11.60	8–12	[82]
2013	PVDF	4.0 wt% N-doped CNT	0.001	1.1	5.7	8–12	[83]
		4.0 wt% undoped CNT	1		17.7		
2008	PA	10 wt% MWCNT	10	—	25.1–25.8	8–12.4	[84]
					20.1–20.6	0.1–1	
2011	Epoxy	5 wt% MWCNT	0.001	0.1–0.4	1.90	1–5	[85]
			0.01	0.8–2.6	10.47		
2014	PDMS	2.5 wt% CNT/G	—	2.5	4.5	8–12	[86]
		5 wt% CNT/G			6.5		
		10 wt% CNT/G			7.9		
2009	PMMA	10 wt% MWCNT film	1.5	0.30	40	8–12	[87]
		10 wt% MWCNT bulk	1.6	1.1	30		
2018	Epoxy	1.0 wt% CNT	—	9.0	−22 (reflection)	8–12	[88]
2016	Epoxy	4.0 vol% MWCNT	—	2.0	44	7–12	[89]
2013	Epoxy	25 wt% MWCNT	100	100	23	8–12	[90]
	PMMA	25 wt% MWCNT	—		32		
2016	Epoxy	1 wt% functionalized MWCNT	—	5	51.72	8–12	[91]
2010	Epoxy	5 wt% MWCNT	0.06	10.16	—	8–12	[92]
		5 wt% SWCNT	0.12				
2011	Epoxy	3 vol% MWCNT	400	2	51.1	8–12	[93]
2019	Epoxy/NCCF	2.35 vol% CNT	0.091	2	40.8	8–12	[94]
2019	PTT	3 wt% MWCNT	25.4	2	38	2.65–3.95	[95]
2012	PANI	25 wt% SWCNT	0.1	2	31.5	2–18	[96]
2007	PMMA	4.76 wt% MWCNT	—	1	28.76–32.06	2–18	[97]
2017	NR	5 wt% MWCNT	100	2.6	43.7	8–12	[98]
2016	EVA/UHMWPE	7 wt% CNT	108.5	2.1	57.4	8–12	[99]
2018	PDMS	<1.0 wt% CNT	—	2	46.3	8–12	[100]
2016	Epoxy	2 wt% CNT	253.4	2	68	0.05–18	[101]
2016	PLLA	10 wt% MWCNT	3.4	2.5	23	8–12	[102]
2005	PS	7 wt% MWCNT	—	—	18.56	8–12	[103]
2017	PMMA	7 wt% MWCNT	—	2.5	13.1	8–12	[104]
2017	HDPE	3.39 vol% CNT		0.58	27.1	8–12	[105]
2019	$Ti_3C_2T_x$	3 wt% CNT	943	3	103.9	8–12	[106]
2010	PCL	1.38 wt% CNT	—	30	45	7–35	[107]
2007	PCL	1 wt% CNT	1.8	30	38	0.4–40	[108]
2009	PMMA	4.76 wt% CNT (*in situ*)	—	1	18	2–18	[109]
		4.76 wt% CNT (*ex situ*)			15		

GTR, ground tire rubber; ABS, acrylonitrile butadiene styrene; EVA, ethylene vinyl acetate; PVDF, polyvinylidene fluoride; PMMA, poly(methyl methacrylate); PVC, polyvinyl chloride; PS, polystyrene; PC, polycarbonate; PCL, polycaprolactone; HDPE, high-density polyethylene; PLLA, poly (L-lactic acid); RET, ethylene terpolymer; PDMS, polydimethylsiloxane; UHMWPE, ultrahigh-molecular-weight polyethylene; NR, natural rubber; NCCF, nickel-coated carbon fiber; PTT, polytrimethylene terephthalate; PA, polyacrylate; PP, polypropylene; PEDOT, poly(3,4-ethylene dioxythiophene); PU, polyurethane; PLA, polylactic acid; PES, polyethersulfone; PEI, polyethylenimine; PVA, polyvinyl acetate; SGM, solid glass microsphere; HGM, hollow glass microsphere; SMP, shape memory polyurethane; EMA, ethylene methyl acrylate; PE, polyethylene; wt%, weight percentage; vol%, volume percentage; phr, parts per hundred.

Radiated interference includes the radiation formed by a device that is propagated through the air away from the device. Conductive interference is formed when radiation from internal devices is propagated through a power or signal conductor and can be problematic because the entire power distribution network is

connected through power cords. EMI occurs in the frequency range of 10^4–10^{12} Hz in the EM spectrum. Hence, EMI can be prevented by placing a shielding material between the source and the device. SE is defined as the ratio of the incident radiation power to the transmitted power and is expressed in decibel. SE can be calculated as shown in equation (1):

$$\begin{aligned} \mathrm{SE} &= 10 \log (P_{\mathrm{in}}/P_{\mathrm{out}}) = 20 \log (E_{\mathrm{in}}/E_{\mathrm{out}}) \\ &= 20 \log (H_{\mathrm{in}}/H_{\mathrm{in}}), \end{aligned} \tag{1}$$

where P_{in}, E_{in}, and H_{in} are the power, electric, and magnetic field intensities incident on the shield, respectively, and P_{out}, E_{out}, and H_{out} are the power, electric, and magnetic field intensities transmitted through the shield material, respectively. A higher EMI SE level indicates that a lesser energy is transmitted through the shield material. A shielding material with 20 dB EMI SE can block 99% of the incoming radiation; hence, this value is required for commercial applications [110,111].

The common EMI shielding measurement techniques are the open-field/free space method, the shield box method, the shielded room method, and the wave guide method. The most favorable method for EMI shielding testing is the wave guide method. This method involves plane wave EM radiation measurements. A reference test sample is mounted on a specially designed holder, which ranges accordingly to the band frequency as presented in Table 2, and the received voltage is recorded at multiple frequencies. The loaded sample is then mounted in the place of the reference sample, and the same measurements are recorded. The ratio of the powers received by the reference and load samples gives the SE of the load material as shown in equation (1). The major benefit of this technique is that the results obtained from different laboratories are comparable, and it can resolve the data into reflected, absorbed, and transmitted components [69,70]. The co-axial method provides comparable results obtained from a different workstation. The American Society for Testing and Materials (D4935-99) has standardized the coaxial transmission line technique as a recognized standard method for the measurement of the SE of planar specimens [66].

Three mechanisms are involved in complete shielding, namely, reflection, absorption, and MIR, which contribute to the overall attenuation of EMI. Thus, total SE would be the sum of all three terms: $\mathrm{SE} = \mathrm{SE}_R + \mathrm{SE}_A + \mathrm{SE}_M$, where R is reflection, A is absorption, and M is MIR. Reflection is the primary shielding mechanism for highly conductive materials, such as metals, because materials for reflection shield must have free charge carriers (electrons or holes), which can interact with incoming EM radiation. These mobile charge carriers generate impedance mismatch; thus, a large part of the incident wave is reflected. Absorption is due to the interaction of EM radiation with the electric/magnetic dipoles, electrons, and phonons in the solid and can also occur from resistive losses, which consist of transforming EM energy in heat by the Joule effect. Absorption shielding can be increased by enhancing the electrical or magnetic dipoles of the shield material depending on absorption shield thickness. The mechanism of multireflection is hard to interpret and usually inconsequential, because most incident EM waves are reflected from the external conductive surface of the shield material (high mobile charge carriers), and only a few of the penetrating EM waves can be retained for multiple reflections. SE_M is negligible as well when SE_A is greater than 10 dB. The influence is more important while using thin shield materials at low frequency (i.e., below approximately 20 kHz). SE_M is almost invisible as the frequency gets higher, because the ratio between material thickness and skin depth becomes larger as frequency increases [60,87,78] (Figure 1).

EMI shielding is measured by the vector network analyzer (VNA) and the scalar network analyzer (SNA) based on the principle of wave guide techniques. SNA can measure only the amplitude of signals, whereas VNA can measure the magnitude and phases of various signals. Therefore, VNA is the preferable instrument despite its higher cost because it can measure complex signals such as complex permittivity or permeability [112,113].

Several factors, such as electrical conductivity, permeability, electrical polarization, frequency, and thickness, are considered for shielding materials. Based on the EM wave theory, SE_R and SE_A are expressed in equations (2) and (3):

$$\mathrm{SE}_R = 39.5 + 10 \log(\sigma/2\pi f\mu), \tag{2}$$

$$\mathrm{SE}_A = 8.7t(\sigma\pi f\mu), \tag{3}$$

where f, t, μ, and σ are the frequency shielding, thickness, permeability, and electrical conductivity of a shielding material, respectively [110]. A shielding material for EM wave reflection must have high electrical conductivity, whereas a shielding material for EM wave absorption must possess high electrical conductivity and permeability with sufficient thickness [60]. Composite materials may have polarization and charge accumulation at their interfaces because of the electrical conductivity mismatch between the filler and the matrix. Hence, the improved dielectric permittivity of composite materials can improve dielectric loss and polymer

Table 2: Communication devices and their frequency range

Category	Frequency	Name	Application	Ref.
Radio frequency	30–300 kHz	VLF-LF	Marine communication	[114]
Microwaves	300 MHz to 1 GHz	UHF	Telecommunication, microwave oven, mobile phones	[115]
Microwave frequency bands	1–2 GHz	L Band	Mobile phones, wireless LAN, radars, GPS	[116]
Microwave frequency bands short wave	2–4 GHz	S Band	Bluetooth	[117]
Microwave frequency bands	4–8 GHz	C Band	Satellite communication, cordless telephone, Wi-Fi	[118]
Microwave frequency bands	8–12 GHz	X Band	Satellite communication	[110]
Microwave frequency bands	12–18 GHz	Ku Band	Satellite communication	[111]
Microwave frequency bands	18–27 GHz	K Band	Satellite communication	[119]
Microwave frequency bands	27–40 GHz	Ka Band	Satellite communication	[113]
Microwave frequency bands	40–75 GHz	V Band	Military and R&D	[112]
Microwave frequency bands	75–110 GHz	W Band	Military and R&D	[120]

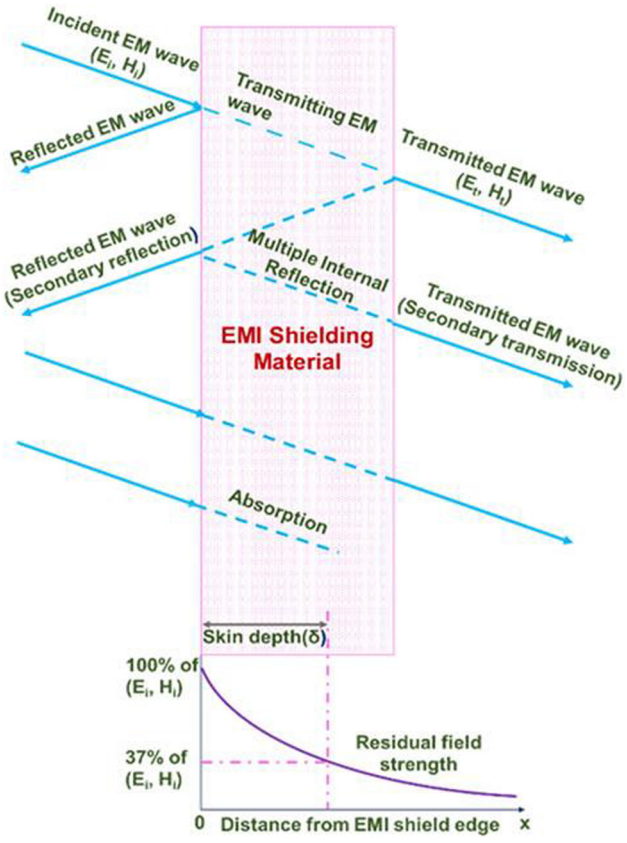

Figure 1: Pictorial depiction of the EMI shielding mechanism and skin depth of an EMI shielding material [60].

composite materials with high dielectric value could be good EM wave absorbers [48]. Polarization composite can be enhanced by the orientation and the type of fillers because nanostructured fillers decrease the eddy current losses and substantially improve permeability. Permeability is an important shielding parameter, because high permeability or magnetic loss is good for EM wave absorption. EMI SE also depends on the radiation frequency as SE_A increases with the increasing radiation frequency [76]. The thickness of the material is important as EMI SE increases with the increasing material thickness. The size and the aspect ratio of fillers have an impact on EMI SE as a high aspect ratio of CNT, which reduces intercontact resistance, therefore provides higher electrical conductivity [74]. Therefore, several factors, including electrical conductivity, permittivity, permeability, filler size, and the thickness of the shielding material, influence EMI SE.

3 Classification of EMI according to application frequency

Article 1.166 of the International Telecommunication Union's Radio Regulations define EMI as the effect of unwanted energy because of one or a combination of emissions, radiations, or inductions upon reception in a radio communication system manifested by performance degradation or the misinterpretation or loss of information that could be extracted in the absence of unwanted energy with mathematical simplicity. Details about communication devices according to their working frequency range are presented later.

4 CNT–reinforced polymer composites for EMI shielding

In the previous section, we have discussed many factors on EMI determination, but electrical conductivity and

permeability are the main parameters for the shield. Polymer hybrid materials have attracted the increasing research interest because of their excellent stability, light weight, flexibility, corrosion resistance, and easy processing. Thus, these materials can replace metals, which have high density and low flexibility. The development of polymer composites with CNTs is presented in this section.

CNTs are rolled up in the form of cylindrical carbon molecules with sp^2 bonds with a very high aspect ratio because of their small diameter. CNTs have extra advantages over conventional carbon fillers, and high EMI SE could be easily obtained at a relatively low CNT percentage filling when composited to polymers because of their low weight, small diameter, high aspect ratio, high electrical conductivity, easy percolation, and good mechanical strength. CNTs form a 3D conductive network within the matrix; thus, electrons can tunnel from one filler molecule to another to overcome the high resistance formed by the insulating polymer matrix. These allotropes can be constituted of a single hollow cylinder, that is, single-walled carbon nanotube (SWCNT), or of a collection of graphene concentric cylinders, that is, multi-walled carbon nanotube (MWCNT) [121]. Polymers are divided into two types: ICP and conducting polymer composite (CPC).

4.1 ICP–CNT composite for EMI shielding

ICPs generally known as "synthetic metals" are organic polymers that possess electrical, magnetic, and optical properties typical of metals and semiconductors while retaining their mechanical property, processability (compared with carbons) with low density (~1.1–1.3 g/cm^3 compared with metals, e.g., ~9.0 g/cm^3 for copper or ~7.87 g/cm^3), and corrosion resistance (compared with metals). Intrinsic conductivity in the field of microwave absorption (100 MHz to 20 GHz) makes ICPs a viable material. Examples of organic conductive polymers include polyacrylate, PANI, PPy, and poly (3,4-ethylene dioxythiophene). CPC has come into existence since the 1950s. CPC has the resistivity of metallic conductor (10^{-7} W m) and thus can be an excellent insulating material for EMI shielding. CPC is also lightweight and has ease of shaping, corrosion resistance, and appropriate electrical and dielectric characteristics to prevent ESD, disturbance, and interference between electronic systems. In the past decade, carbon black particles and CFs have been the most commonly used conductive filler components because of their high surface area and high charge transfer capabilities. The research area has taken a new lead since the advent of nanocarbons, such as CNT, because of the rapid development of material science and engineering. The nanocluster is an ultra-fine particle with nanometer dimensions (SWCNT < 1 nm and MWCNT > 100 nm) and has characteristics that are size dependent and are different from those of the atomic and bulk materials. CNTs are widely used as effective fillers in ICPs and CPCs because of their large surface area, high aspect ratio, high electrical conductivity, and easy processability [122]. Examples of CPCs are epoxy, acrylonitrile butadiene styrene, ethylene vinyl acetate (EVA), polyvinylidene fluoride (PVDF), poly(methyl methacrylate) (PMMA), polyvinyl chloride, polystyrene (PS), and polycarbonate (PC) [40].

4.2 ICP composite for EMI shielding

Yuan et al. found that 25 wt% SWCNT reinforced in PANI can give rise to an absorption dominant of 31.5 dB at 18 GHz frequency because of the improved connectivity and electrical conductivity of the SWCNT–PANI composite. Strong electrostatic attraction force enhances the interface contact in the composite and helps in forming an extensive conductive network [96]. Saini and Choudhary found that using MWCNT instead of SWCNT for reinforcement in PANI can cause energy loss because of the dielectric dissipation caused by the MIR effect and the absorption by PANI coating. The MIR effect is due to the presence of highly reflecting MWCNT, which leads to multiple EM radiation scattering and results in the multiple passes of radiation between randomly distributed MWCNTs. Therefore, the increase in the total number of reflecting MCNT planes that are present between two shields leads to an increase in absorption as the MWCNT content increases [49]. ICP–CNT composite made with *in situ* polymerization has more advantages over other composites, such as polyethersulfone and polyethylenimine, which are made through other processing methods [57]. The β-alignment of CNTs is conducive to exploit their special radial properties, such as sieve effect dominated by their serial diameter and field effect from their excellent conductivity, in a normal plane. A highly conducting PANI coated with MWCNT through *in situ* polymerization had shown improvement in EM absorption (from −27.5 to −39.2 dB). The interconnecting bridge between the various conducting

grains of PANI, which are coated by individual MWCNT, increases the coherence between the chains, which enhances the interchain transport. Dipole polarization and interfacial polarization, along with the reduction in surface reflectivity because of skin effect, have led to enhanced EM absorption. The same group reported that the electrical conductivity of PANI–MWCNT composite (19.7 S/cm) is higher than those of MWCNT (19.1 S/cm) and PANI (2.0 S/cm) because of an increase in the coherence or coupling between the chains, and this increase in electrical conductivity leads to the enhancement of the interchain transport. The increase in coherence is because polymerization takes place on the surface at a certain critical amount of MWCNT and leads to a uniform coating of PANI over MWCNT. This enhancement will eventually facilitate the intertube charge transport by reducing interfacial contact and tunneling resistance [4].

4.3 CPC–CNT composite for EMI shielding

The processing method for CPC matrix is quite crucial because electrical and EMI properties can be enhanced only with the amount and ways the filler is distributed in the polymer. Yuen et al. fabricated the MWCNT-based composite with PMMA using *in situ* and *ex situ* polymerization. Their findings showed that the composite prepared by the *in situ* method had better adhesion of MWCNT to PMMA and therefore gained superior performance than the composite prepared by *ex situ* polymerization. The EMI SE for MWCNT/PMMA (*in situ*) with 4.76 wt% MWCNT exhibits EMI SE in a wide frequency range (max SE of 32.06 dB at 2.18 GHz and leveled high value of 28.76 dB at 7.10 GHz). The surface electrical resistivity of the composite (*in situ*) decreased by 13 orders of magnitude from $9.75 \times 10^{15}\,\Omega$ (neat PMMA) to $5.92 \times 10^{2}\,\Omega$ (4.76 wt% MWCNT) [97]. The aspect ratio of CNT is the main parameter to improve the performance of a composite matrix. A study [79] synthesized three different SWCNTs, namely, (i) SWCNT-long, which exhibited the largest bundle length/diameter aspect ratio; (ii) SWCNT-short, which exhibited a smaller aspect ratio; and (iii) SWCNT-annealed (obtained after annealing SWCNT-short), which exhibited improved conductivity despite the smaller aspect ratio because of the removal of wall defects and functional groups. The SWCNTs were composted with epoxy polymer, and SWCNT-long showed the highest EMI SE, which is 49 dB, at 15 wt% loading [79]. This result proves that the high aspect ratio of SWCNT is the main parameter needed to obtain high EMI SE in the experiment of SWCNT–epoxy composite. Semi-crystalline polymers, such as ethylene methyl acrylate (EMA), have also been used in shielding applications because of their excellent mechanical, thermal, and chemical properties. EMA/MWCNT composite with 10 wt% MWCNT content displays a closely packed conductive structure, which leads to an EMI SE of 22 dB at 10 GHz [28]. A number of CNT composites prepared by *in situ* polymerization, such as CNT/polyurethane (PU) composites [66], poly(2,5-benzoxazole)/MWCNT composites, have remarkably improved dielectric permittivity from 4 (polymer matrix) to 65 with the incorporation of 5 wt% MWNT [123]. PI/SWCNT composites with 10-fold enhanced that the electrical conductivity have also gained a low φ_C (around 0.05 wt%) [124]. *In situ* polymerization can help polymers that are difficult to dissolve and melt to form composites. Shape memory polymer-based composites possess superior characteristics such as easy resilience, light weight, and capacity to be molded at a superficial degree. MWCNT/PU composite exhibits 35 dB for K band, 52 dB for Q band, and 60 dB for V band at 6.7 wt% MWCNT and 3 mm thickness. A thickness of 0.5 mm was considered in another experiment under the same frequency condition, and the results showed that composites with 3 mm thickness have better EMI SE than those with 0.5 mm thickness. Although the electrical resistivity of CNT/PU decreases with the increasing CNT weight fraction, the φ_C is about 10 wt%, which is quite high [125]. Thus, a high amount of CNT filler loading is needed to enhance the EMI shielding of solid composites, and this finding is quite troubling as industries are aiming for lightweight materials to ease the processing and decrease the cost.

Several approaches can produce lightweight electrically conductive materials with high EMI shielding capabilities. Most polymers have density values in the range of 0.9–1.2 g/cm^3, which is remarkably lower than the density values of conducting metals, such as copper (8.96 g/cm^3). The density of the conducting fillers will increase with the addition of conducting fillers. This occurrence explains why CNT is one of the preferable conducting fillers as its density is less than 1.6 g/cm^3. Therefore, innovative methods have been developed to incorporate porosity in the material to decrease the density of the composite while obtaining high EMI shielding capability. Currently, lightweight and highly flexible materials are being targeted to obtain high EMI SE. Crosslinking and the use of foam/sponge or

segregated structures are some of the ways to obtain lightweight and flexible materials. Uniquely structured ICPs and CPCs, such as double percolation, layer-by-layer assembly, and multilayer, have enhanced the EM absorption [81].

5 Crosslinking composite structure

The composition of SWCNT with PU composite has obtained 16–17 dB over the X-band frequency range at 20 wt% through simple physical mixing, which costs less and has ease of processing. The performance of the composite is mainly the reflection from highly conducting SWCNT network at lower filler loading; however, the increased imaginary part of the dielectric permittivity leads to absorption-dominated SE at higher filler loading (>10 wt/%). Moreover, the composite produces strong microwave absorption by using cross-linked PU instead of normal PU as a matrix for SWCNT reinforcement because of the high dielectric loss of 22 dB at 8.8 GHz with 5 wt% filler loading [66].

5.1 Segregated and double percolation composite structure

Other than cross-linked polymer/CNT composites, many segregated CNT/polymer composites have been developed for high-performance EMI shielding [21,59,98,126–129]. Li et al. studied the EMI effect of the arrangement of CNT in segregated and whole natural rubber (NR). CNTs tend to "squeeze" along specific paths and isolate to the periphery of NR domains rather than to randomly distribute in the whole NR matrix. The whole NR matrix tends to restrict the diffusion of CNT and NR domains and results in selective distribution. However, in segregated structure, the NR domains without CNTs are described as "excluded volume," which pushes CNTs to the boundaries of NR domains to form the localized CNT conductive network. This unique structure decreases the overall CNT loading and creates multiple conductive surfaces that can effectively shield EM fields. The segregated structure has obtained 20 dB at 1.0 wt% CNT unlike conventional CNT/NR composites, which require 5.0 wt% CNT to obtain 20 dB [98].

The unique segregated structure can be considered as a shielding material with numerous core–shell units, in which NR domains (cores) are encapsulated by highly conductive CNT layers (shells). The segregated core–-shell units provide numerous interface areas, which are conducive to enhance SE_A, SE_R, and SE_M. Consequently, microwaves hardly escape before being absorbed and dissipated as heat; thus, the material has superior absorbing ability, which is suitable for highly efficient EMI shielding. The segregated structured composites cause high strain tolerance and good flexibility. A highly flexible composite of CNT reinforced with ground tire rubber (GTR) from industrial waste was fabricated for high EMI shielding. The EMI SE of CNT/GTR composite is 66.9 dB with only 5.0 wt% filler loading. The reliability of EMI SE under mechanical deformation is an important indicator for the evaluation of the flexibility of shielding materials. The segregated CNT/GTR composite was still able to fulfill the commercial application EMI SE (20 dB) by obtaining an average of 20.9 dB despite having performed repeated cyclic bending to the radius of 2.0 mm for 5,000 times. The cyclic bending–release test further demonstrates that the composite's resistance maintains its high stability with only 4% change even after 5,000 cycles; thus, high cyclic reliability is responsible for superior EMI SE reliability [10]. This finding indicates the great potential of such composites as flexible shielding materials in future flexible electronics especially for use on curved surfaces and movable parts (Figure 2).

Another group further developed a very flexible segregated conductive CNT with additional hybrid stainless steel fiber (SSF) in the PPy composite via simple melt mixing. The combination of two hybrid nanofillers (3.5 vol%) gives an EMI SE of 70.43 dB on the absorption-dominant part because of the synergistic effect of the high intrinsic conductivity of SSF and the enormous surface area of CNT [21]. Wang et al. explored the synergetic effect that leads to the highest attenuation of EMI through the absorption-dominant part and found that this attenuation is attributed to the back-and-forth oscillation of ions, the rotation of induced/permanent dipoles, the high permittivity provided by immobilized ions and the dipoles of CNT and polymer, and the interconnected network of the CNT [129]. The segregated structure tends to have a direct influence on the electrical conductivity of composites based on φ_C. The presence of 1D CNT plays the role of a "bridge," which forms well-developed conducting channels for electron transport compared with the single graphite flake-filled composite. The transport mechanism of the hybrid manifested favorable conducting contacts with higher geometrical dimensionality where the amount of surface within the hybrid filler networks increases. This

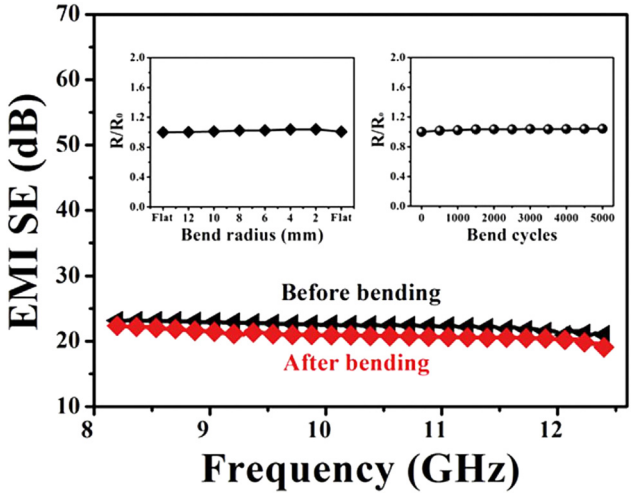

Figure 2: EMI SE of the 5.0 wt% CNT-loaded composite (0.4 mm thickness) before and after repeated bending to the radius of 2.0 mm for 5,000 times. Left inset shows the variation in the normalized resistance (R/R_0) of the 5.0 wt% s-GTR composite as a function of the bending radius. Right inset shows the R/R_0 as a function of bending cycles (radius of 2.0 mm) [10].

mechanism results in relatively low contact resistance and thus improves the electrical conductivity of the composites [127]. Graphite–CNT hybrid employed into ultrahigh-molecular-weight polyethylene (UHMWPE) exhibited an electrical conductivity of 195.3 S/m and an EMI SE of 81 dB in the X-band frequency range [51]. CNTs function as an interfacial linker and are localized at the boundaries of polymers in most of the segregated CNT/polymer composites; thus, the presence of CNTs results in highly conductive percolated conductive network in the composite sample. The φ_C in the composite structure is the key parameter in judging whether the obtained composite structure has the continuous conducting network or *vice versa*. The composite's electrical conductivity and EMI SE increase as the filler content increases above the φ_C. The as-obtained percolated network of CNTs in segregated composites gives high enough electrical conductivity and subsequently results in high EMI SE. The double percolation structure of CNT/EVA/UHMWPE composite with only 7 wt% CNT gives an EMI SE of 57.4 dB, which is higher than that of single-percolated composite [99]. φ_C could be obtained at very low CNT content, which is quite advantageous in forming the interconnected network between CNT and polymer for electrical conductivity and increasing the EMI SE of the composites. Zhang et al. obtained the φ_C at very low MWCNT content (0.019 vol%) with an electrical conductivity of 25 S/m and an EMI SE of ~30 dB. These values of electrical conductivity and EMI SE are 36% higher than those of the sample obtained at 0.8 vol% MWCNT loading. Another important highlight in this research is the skin depth (δ), which is related to the electric field and magnetic field of the materials and is used to evaluate the critical thickness for electrical conduction and EMI shielding. High-performance EMI shielding occurs at the thickness of the samples beyond δ. A higher δ value indicates poor EMI shielding. The δ values at 8.2 GHz at 0.8 vol% segregated and randomly distributed MWCNTs are 1.11 and 32.09 mm, respectively. The findings prove that the segregated MWCNT exhibits the highest efficiency for the attenuation of microwaves compared with the randomly distributed MWCNT [130]. The high EMI SE value is the result of the synergistic effect from the formation of the extended conjugation network with CNT bridging the gaps between the graphene sheets and inhibiting the face-to-face aggregation of graphene sheets. Thus, we can prove that the segregated structured CNT–polymer composites minimize the stacking effect and aggregation of graphene sheets and eventually increase the polymer contact area and interfacial interactions, which lead to a synergetic improvement in composite properties.

5.2 Foam, sponge, and aerogel composite structures

The EMI SE of carbon foams is closely correlated with the char yield of polymer precursors and demanding carbonization conditions. From the viewpoint of lightweight requirement, assembling 1D CNT and 2D graphene sheets into 3D macroscopic structures (e.g., sponges, foams, and aerogels) has emerged as an efficient approach. Lightweight porous foam/sponges/aerogels could give much higher EMI SE because of the multiple EM-wave reflection within the foam's pore wall compared with a thin film of bulk EMI shielding materials. The spherical air bubbles in the foam structure enhance the attenuation of incident EM waves by MIR and the decay between the cell wall and nanofillers, which result in the absorption and dissipation of microwaves as heat before escaping from the materials [100,102] (Figure 3).

Flexible CNT sponges with a density of 10.0 mg/cm^3 were synthesized through chemical vapor deposition and composed of self-assembled and interconnected CNT skeleton. The freestanding CNT sponges have a high EMI SE of 54.8 dB in the X band. The CNT/polydimethylsiloxane (PDMS) composite has still exhibited excellent EMI SE (46.3 dB) at the thickness of 2.0 mm at CNT filler loading of less than 1.0 wt% [100]. This microcellular structure works well for insulating polymer, such as

epoxy, with the assistance of metallized polymeric sponges known as metal-plated foam. Xu et al. fabricated hybridized epoxy composite foams by impregnating expandable epoxy/MWCNT/microsphere blends into a preformed, highly porous, and 3D silver-coated melamine foam (SF) sponge. The highly conductive SF (5×10^3 S/m) resolved the problem of foam reduction in highly filled epoxy blends and provided channels for rapid electron transport. This occurrence can be proven as the conductivity of the reinforced SF–epoxy foam (1.21×10^2 S/m) is about 15 orders of magnitude higher than that of the unalloyed epoxy foams. The φ_C obtained was low as well with 0.5 wt% loading. The EMI SE of 68.1 dB was achieved with only 2 wt% MWCNT and 3.7 wt % silver because of the synergy of MWCNT and SF compared with unalloyed epoxy foams (10.4 dB). MWCNT was used to offset the loss of conductive pathways caused by the crystal defects in the silver layer and the insulating epoxy resin [101] (Figure 4).

The solid bulky composite tends to possess high SE with the increasing weight percentage, but its mechanical properties and process ability tend to decrease. Foaming is one of the best techniques to obtain low-density EMI shielding materials because of its ease in processability and overall shielding performance. MWCNT/biodegradable poly (L-lactic acid) (PLLA) composite foam with 10 wt% MWCNT has displayed outstanding properties, such as low density (0.3 g/cm^3), high compressive strength (54 MPa), low thickness (2.5 mm), an electrical conductivity of 3.4 S/m, an EMI SE of 23 dB, and an average specific EMI SE of 77 dB cm^3/g in the X band; these properties show its potential for high EMI shielding applications in the electronics, packaging, and automobile sectors [102]. Meanwhile, the EMI performance of CNT foam and carbon nanofiber (CNF) foam-reinforced PS composite over the X band was investigated. A specific SE of 33.1 dB cm^3/g was achieved by the PS foam with 7 wt% CNT, which is comparable with that of the PS foam with 20 wt% CNF; thus, CNTs are better at EMI shielding than CNFs. These differences result from the fact that smaller CNTs provide a larger interfacial area; therefore, the number of conductive interconnected nanotubes increases. The larger aspect ratio of CNTs help to create extensively continuous networks that facilitate electron transport in the foam composite with very low nanotube loading [103].

The difference in the EMI performance between solid and foamed composites is important. Zhang et al. fabricated the PMMA foam reinforced with iron oxide (III) decorated with MWCNT (Fe_3O_4–MWCNT) via supercritical carbon dioxide foaming process to form a composite foam with a density of 0.22–0.38 g/cm^3. The composite foam was compared with solid composite, and the results showed that the composite foam benefits from the existence of microcellular structure and Fe_3O_4–MWCNT hybrids; thus, the specific EMI SE of the fabricated foams is remarkably higher (50 dB cm^3/g) than that of the solid composite (15 dB cm^3/g) at 7 wt% MWCNT [104]. The similar result was obtained with CNT/high-density polyethylene (HDPE) foam, which has 21.2 dB at low φ_C of 1.66 vol%, whereas solid CNT/HDPE requires a higher CNT content of about 2.31 vol% [105]. Foamed composite greatly improves electrical conductivity than unfoamed composite. For polycaprolactone (PCL)/CNT composite, 0.249 vol% foamed MWCNT exhibits a conductivity twice that of the unfoamed sample filled with 0.48 vol% MWCNT because the introduction of air on foaming leads to a lower dielectric constant. The EMI SE of foamed 0.249 vol% MWCNT is triple than that of the unfoamed sample filled with 0.48 vol% MWCNT because of foaming [75] (Figure 5). The main advantage of using foaming is that biodegradable polymers, such as PLLA, whose derivatives are from renewable sources such as corn and sugarcane, and can

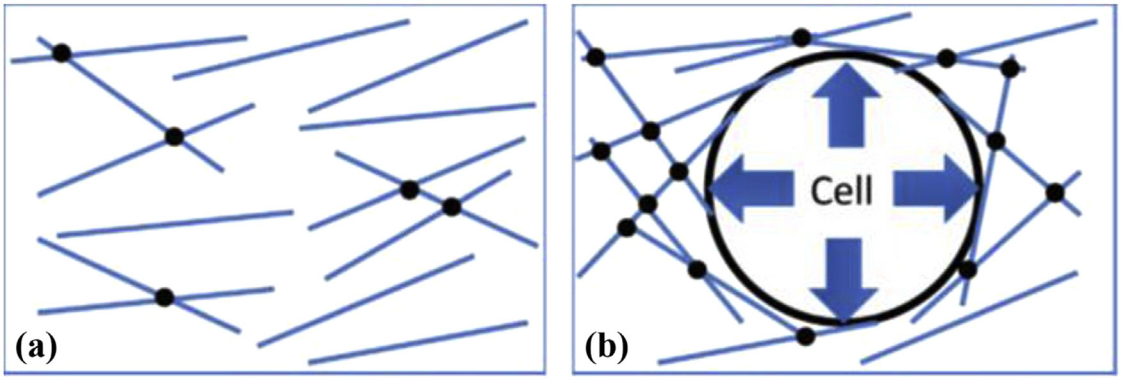

Figure 3: Schematic illustration of the effect of cellular air porosity on the interconnectivity of fibers. Fiber alignment (a) before and (b) after cell formation [62].

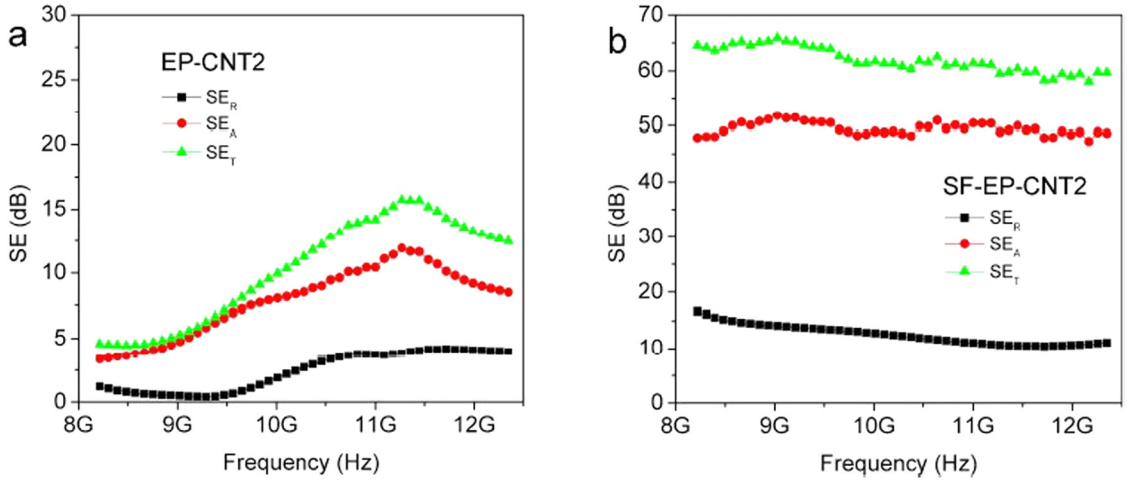

Figure 4: Variations in the total EMI SE, SE_A, and SE_R of the (a) EP-CNT2 and (b) SF-EP-CNT2 samples over the X band [101].

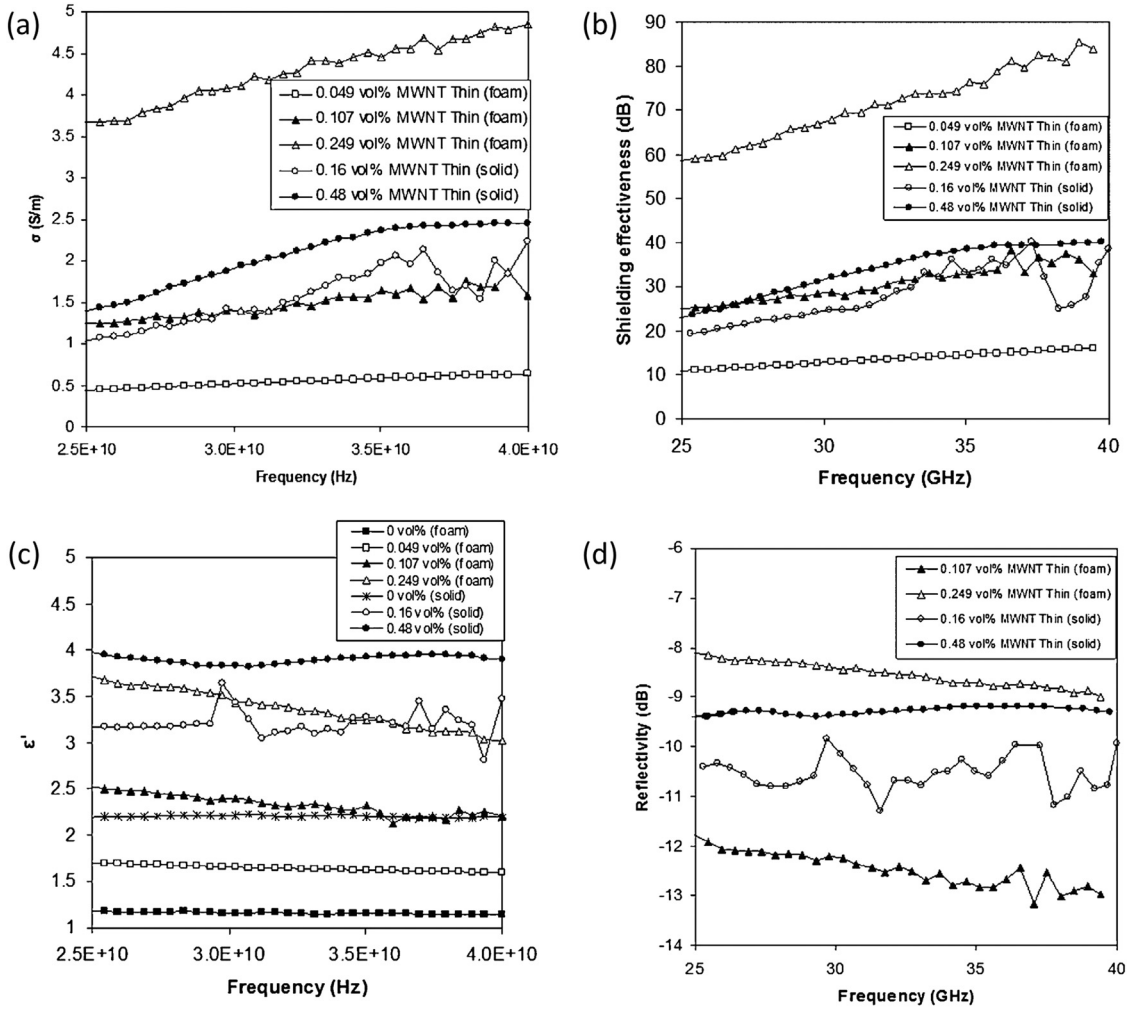

Figure 5: Electromagnetic properties of foamed and unfoamed MWNT/PCL nanocomposites: a) electrical conductivity, (b) SE, (c) dielectric constant, εr and (d) reflectivity, R [75].

be fabricated with CNT and thus exhibit high EMI shielding. A similar occurrence has been observed in traditional petrochemical-derived plastic CPC, such as PMMA [29], PC [44,80], PDMS [81], and epoxy [89,93,94]; thus, the widespread use of these CPC foams as EMI shielding materials in practical applications has expanded. Besides, new 2D materials based on transition metal carbides and/or nitrides, known as MXenes, have recently showed promising results in EMI shielding. MXenes have a formula of $M_{n+1}X_nT_x$, where M is an early transition metal; T is a terminating group, such as O, OH, and/or F; X is a carbon and/or nitrogen; and $n = 1$, 2, or 3. MXenes were first discovered in 2011 by selective etching and the delamination of their layered MAX phase. Similar to CNT, MXenes possess excellent electrical and thermal conductivity, high aspect ratio, good mechanical properties, oxidation resistance, and hydrophilic surface that allows processing from aqueous solutions [131]. A 3D porous $Ti_3C_2T_x$/CNT hybrid aerogel via the bidirectional freezing method was fabricated, where Ti refers to titanium. The synergism of the lamellar and porous structures of MXene/CNT hybrid aerogels has shown excellent electrical conductivity (9.43 S/cm) and superior EMI SE (103.9 dB) at 3 mm thickness at the X band. CNT reinforcement in MXene/CNT hybrid aerogels enhances the mechanical robustness and increases the compression modulus by 96.61% relative to pristine MXene aerogel. The first reflection occurs before absorption when EM waves impinge on the shielding material, and part of the EM waves is immediately reflected from the surface owing to a large number of charge carriers from the highly conducting surface (blue arrows). Induced local dipoles from termination groups help with the absorption of the incident waves passing through the MXene structure (green arrows). The surviving EM waves encounter the next barrier layer after passing through the first layer of $Ti_3C_2T_x$, and the phenomenon of EM wave attenuation is repeated. Transmitted waves with lesser energy are then subjected to the same process when they encounter the next MXene flake, which gives rise to multiple internal reflections (orange arrows), as well as more absorption. The intensity of an EM wave is substantially decreased each time it is transmitted through an MXene flake and results in the overall attenuation or elimination of the EM wave. Thus, such laminated kind of $Ti_3C_2T_x$/CNT hybrid aerogel provides the multilevel shield efficiency ability [106] (Figure 6).

5.3 Multi-layered composite structures

Another alternative to further improve EMI SE is by preparing multilayered structures. Two different cases must be distinguished for multilayered structures. The first one comprises stacking different layers of polymer composites with the same concentration of carbon particles. This strategy works well for PMMA [132] and epoxy [85] composites, as the impact on absorption is dominate and results in higher SE/reflectivity ratio despite the presence of multireflection, which increases the total reflection. The second case would be gradually increasing the carbon filler layer by layer to avoid the presence of an interface between two mediums with large dielectric constant difference, which consequently limits the reflectivity at each interface. A model was built to validate this theory through the face-to-face assembly of three slices of foams with the increasing CNT concentrations and different thicknesses: 0.5 wt% (11 mm), 1 wt% (2 mm), and 2 wt% (17 mm). The average CNT concentration in this three-layered structure was 1.38 wt% with a total thickness of 30 mm. The thickness of the first layer (lowest CNT concentration and dielectric constant) is about one third of the total thickness to ensure the smooth penetration of the signal into the composite, whereas the second layer has intermediate concentration function to match the low dielectric constant of the first layer to the higher dielectric constant of the third layer. The third layer was thick (two thirds of the total thickness with highest CNT concentration) to dissipate the residual radiation power. The bold solid curve shows that the EMI SE of the three-layered foam is comparable with that of a monolayer foam with the same thickness and similar CNT concentration (1 wt%, dashed curve). The total reflection by the multilayer was decreased by at least 5 dB or by approximately 70% compared with the monolayer (1 wt%, dashed curve). Moreover, the substantial reduction in reflection was observed over a broad frequency range (restricted to 28 GHz because of experimental constraints) and is remarkable when compared with the reflection by the Salisbury screens, which is lower than −10 dB over less than 2 GHz [107]. Notably, microwave is attenuated by absorption when reflected at any one of the intermediate interfaces; therefore, this material works well as a radar-absorbing material (RAM), which targets more signal absorption rather than reflection (Figure 7).

6 Surface modification of CNT for improving EMI performance

The dispersion of CNT within a polymer matrix remains a problematic task. The main problem with CNT is its tendency to agglomerate and bulk fast. Several attempts

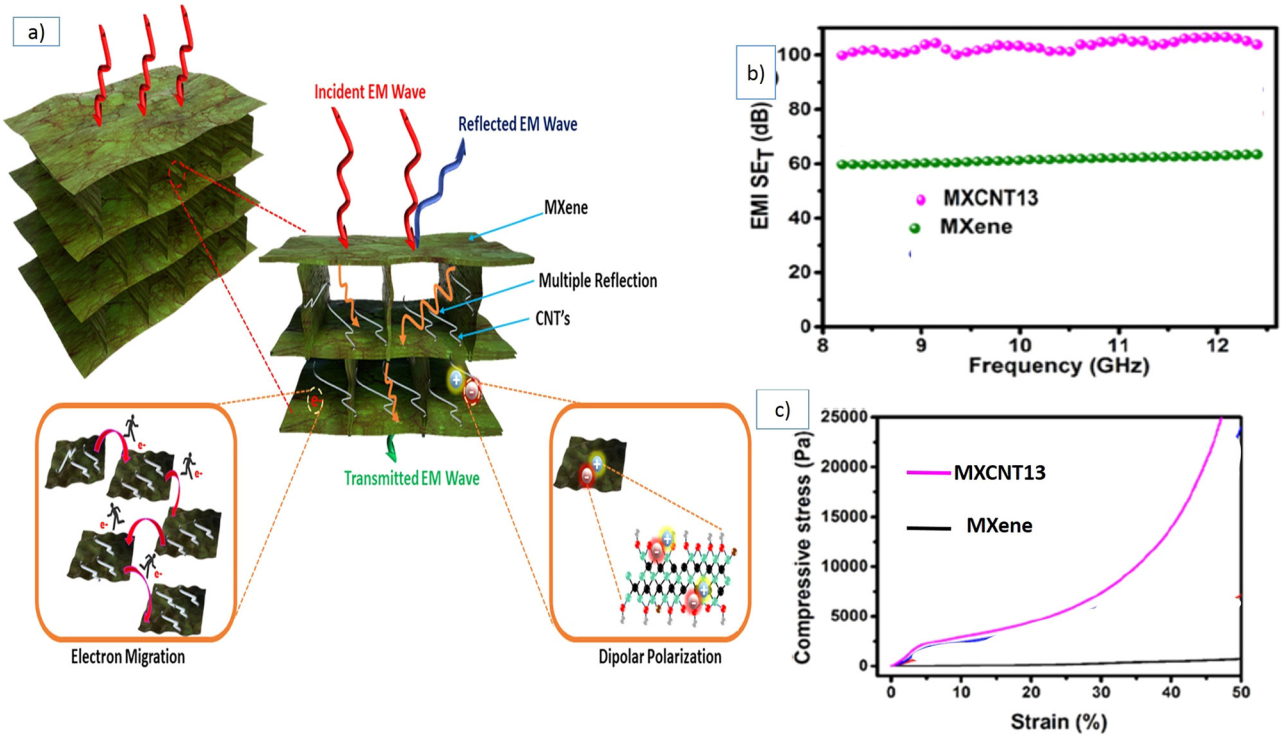

Figure 6: (a) Schematic representation of the possible mechanism of EMI shielding in MXCNT aerogel foam; (b) EMI SE$_T$ of MXene and MXCNT13 aerogels with 3 mm thickness as a function of frequency; and (c) stress–strain curves of MXene and MXCNT13 aerogels [106].

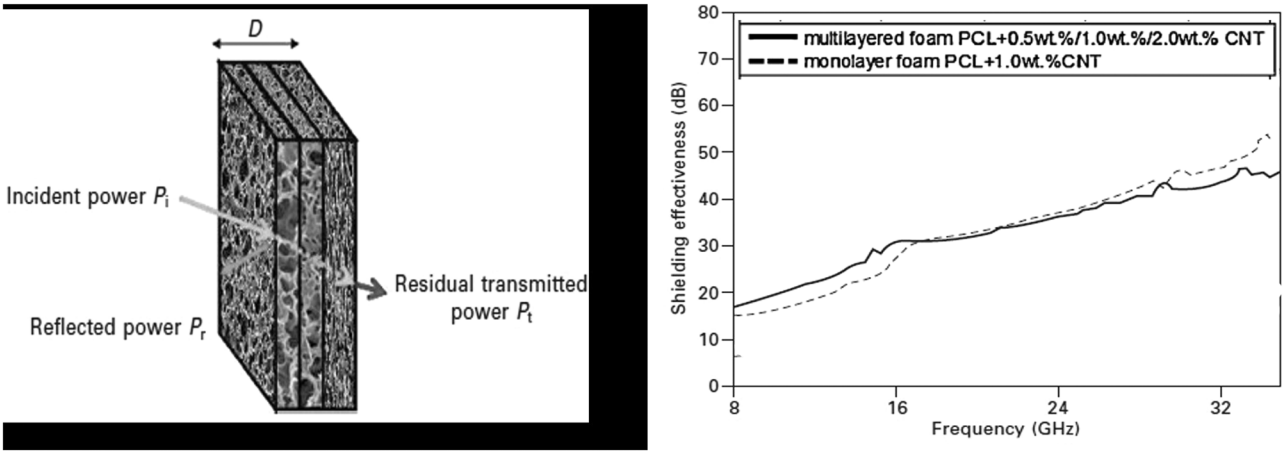

Figure 7: Reflection and SE of a three-layered MWNT/PCL nanocomposite foam (left). SE of a single CNT concentration: 1 wt% (dashed) compared with a three-layered sample with graded CNT concentration (bold lines): 0.5 wt% (11 mm)/1 wt% (2 mm)/2 wt% (17 mm) (right) [107].

have been carried out to overcome this challenge. Thomassin et al. used π–π interactions between the aromatic structure of nanotubes and the –COOH/COH groups of the polymer PCL to obtain a good dispersion of MWCNT. This CNT–polymer composite has exhibited an improved conductivity and an EMI SE exceeding 20 dB [108]. The same group further synthesized the PCL/MWCNT foam structure and produced a much higher EMI SE (~60–80 dB) at very low MWCNT loading (0.25 vol%) when compared with the unfoamed PCL/MWCNT structure [75]. Besides, the functionalization of CNTs improves the dispersibility of CNTs and the EMI SE of the composites. Doping/acidic treatment using solvents, such as nitric acid, sulfuric acid, and hydrogen

peroxide, can be used to introduce oxygen functional group because of the presence of lattice defects in the nanotubes by attacking the cap or the side wall of the nanotubes. Several literature reviews have reported the functionalization of CNT in polymers, such as PVDF [22,47,46], PS [25,53], PANI [49], ethylene terpolymer [56], and epoxy [91]. A nitric acid–modified MWCNT (f-MWCNT) exhibits improved dispersion in PVDF through the formation of chemical bonding between CNTs and PVDF. As a result, this f-MWCNT–PVDF composite showed an absorption dominant EMI SE of 47 dB at the very low MWCNT loading of 0.5 wt% compared with the nonfunctionalized composite, which needs 4 wt% MWCNT to achieve the same amount of EMI SE. Electrical conductivity has increased by almost twice from 3.72×10^{-3} S/cm (4 wt% MWCNT) to 8.72×10^{-3} S/cm (0.5 wt% f-MWCNT) [22]. Therefore, the presence of large lattice defects in the CNTs and high electrical conductivity result in low skin depth and give rise to a high microwave absorption capacity. Besides improving EMI shielding performance, mechanical and thermal properties are also enhanced via acid functionalization. Previous studies showed that adding 0.5 wt% acid-treated CNT results in a 22% increase in Young's modulus and a decrease in the viscoelastic behavior of the PS matrix. Differential scanning calorimetry scans showed a decrease in the glass transition temperature of the PS/CNT composites; therefore, acid medication decreases the filler–filler interaction and results in a better dispersion in the PS matrix [25,53]. Li et al. reported that the presence of f-MWCNT would reduce the activation energy barrier to nucleation and lead to more cell nucleation in the boundary between the polymer matrix and the dispersed filler particles. The average distance between f-MWCNT would be reduced, and effective conducting CNT pathway could be constructed at a lower φ_C [133]. However, doping or acid functionalization might damage the CNT structure and degrade the best intrinsic properties of CNT at the elevated temperature. For instance, the EMI SE of N-doped CNT with PVDF nanocomposite (5.7 dB) is three times smaller than SE value than that of undoped CNT/PVDF (17.7 dB). This finding proves that N-doping conveys a negative effect on the crystallinity, metallicity, aspect ratio, and dispersion state of CNTs and results in poor EMI performance [83]. Therefore, N-doping CNT is detrimental for the EMI shielding applications of CNT/polymer nanocomposites. Thus, efforts have been made to reduce CNT damage. Huang et al. fabricated a composite with maleic anhydride-functionalized MWCNTs (MAH-*g*-MWCNTs) and PMMA. An EMI SE of 11 dB could be obtained at very low loading (~2.44 wt%) because of the good adhesion of Mah-*g*-MWCNTs with PMMA by covalent bonding, which reduces the structural damage in the CNT networks [109]. Noncovalently functionalized MWCNT coated with PANI in the PS composite has microporosity, very low φ_C (0.12 vol% MWCNT), and high permeability. The composite has showed maximum SE_A (–18.7 dB) and little SE_R (–4.6 dB) at 7 vol% MWCNT loading. The mechanism of shielding can be explained in terms of MIR. The presence of pores and highly reflecting MWCNT leads to the multiple scattering of EM wave and loss of energy because of dielectric dissipation. Maximum absorption loss is generated because of high permeability, and this finding can be used in designing futuristic RAM or stealth technology [49].

7 Challenges and future research perspectives

In this review, we highlighted the recent research progress in the advancement of polymer-based materials for EMI shielding. A comprehensive introduction to EMI shielding has been reviewed. The shielding theory and factors contributing to EMI attenuation have been highlighted as well. Then, conducting and nonconducting/insulating polymer and their polymer composites with CNT have been summarized in detail. The composites have been discussed with the emphasis on the roles of the size, shape, and electronic and chemical properties of nanomaterials in tuning EMI shielding properties. A specific correlation between the surface chemical modification or doping with CNT filler materials and the EMI SE of their polymer hybrid has been summarized. Despite the substantial achievement, the fast-growing demand of future EMI shielding requires thinner, lighter, and highly effective polymer hybrids. New materials need to be developed and explored to fulfill the demand by customizing the properties of the polymer/filler. A fundamental understanding of the electronic and structural properties of materials is necessary to optimize the SE of polymer hybrids. The following future research directions are expected to be explored in the nearest time to achieve the targets:

(1) CNT–polymer composite hybrid with titanium carbide-based MXene filler has already exhibited superior EMI shielding. A wide range of MXene materials, which have high conducting properties, is expected to be an excellent selection for EMI

shielding application. Therefore, a huge prospect can be explored in the MXene-based CNT–polymer composite in EMI shielding application.

(2) Polymerization of the surface functional group over the filler is necessary to explore instead of polymer hybrid with bulk mixing. This specific functionalization will be helpful for the minimum sage of the polymer and the better distribution (localized distribution) of the filler than bulk mixing (random distribution) in the composite.

(3) Defect and doping during functionalization greatly control the properties of 1D CNT. Polymer hybrid with tunable defect/doping needs to be studied to further achieve the synergistic effect of defect/doping with the properties of the polymer host.

(4) Similar to monolayer or multilayered foamed structures, hollow-foamed honeycomb can act as a lightweight EMI shielding material. CNT–filled polymer foam in metallic honeycomb reduces the real part of the effective dielectric constant of the hybrid and results in a very high EM absorption in a wide frequency range (>60 GHz) [134]. The suitable pore size and the structure are targeted to maximize MIR and absorption.

Acknowledgments: The study was funded by the Universiti Sains Malaysia (FRGS Grant 203/PAERO/6071409).

Conflict of interest: The authors declare no conflicts of interest regarding the publication of this paper.

References

[1] Yousefi N, Sun X, Lin X, Shen X, Jia J, Zhang B, et al. Highly aligned graphene/polymer nanocomposites with excellent dielectric properties for high-performance electromagnetic interference shielding. Adv Mater. 2014;26(31):5480–7.

[2] Wang C, Chen M, Lei H, Yao K, Li H, Wen W, et al. Radar stealth and mechanical properties of a broadband radar absorbing structure. Composites Part B. 2017;123:19–27.

[3] Sankaran S, Deshmukh K, Ahamed MB, Khadheer Pasha SK. Recent advances in electromagnetic interference shielding properties of metal and carbon filler reinforced flexible polymer composites: a review. Composites Part A. 2018;114:49–71.

[4] Saini P, Choudhary V, Singh BP, Mathur RB, Dhawan SK. Polyaniline–MWCNT nanocomposites for microwave absorption and EMI shielding. Mater Chem Phys. 2009;113(2–3):919–26.

[5] Theilmann P, Yun DJ, Asbeck P, Park SH. Superior electromagnetic interference shielding and dielectric properties of carbon nanotube composites through the use of high aspect ratio CNTs and three-roll milling. Org Electron. 2013;14(6):1531–7.

[6] Park OK, Chae HS, Park GY, You NH, Lee S, Hui D, et al. Effects of functional group of carbon nanotubes on mechanical properties of carbon fibers. Composites Part B. 2015;76:159–66.

[7] Liu Z, Peng W, Zare Y, Hui D, Rhee KY. Predicting the electrical conductivity in polymer carbon nanotube nanocomposites based on the volume fractions and resistances of the nanoparticle, interphase, and tunneling regions in conductive networks. RSC Adv. 2018;8(34):19001–10.

[8] Jiang Q, Wang X, Zhu Y, Hui D, Qiu Y. Mechanical, electrical and thermal properties of aligned carbon nanotube/polyimide composites. Composites Part B. 2014;56:408–12.

[9] Chizari K, Arjmand M, Liu Z, Sundararaj U, Therriault D. Three-dimensional printing of highly conductive polymer nanocomposites for EMI shielding applications. Mater Today Commun. 2017;11:112–8.

[10] Jia LC, Li YK, Yan DX. Flexible and efficient electromagnetic interference shielding materials from ground tire rubber. Carbon. 2017;121:267–73.

[11] Arjmand M, Mahmoodi M, Gelves GA, Park S, Sundararaj U. Electrical and electromagnetic interference shielding properties of flow-induced oriented carbon nanotubes in polycarbonate. Carbon. 2011;49(11):3430–40.

[12] Kar GP, Biswas S, Rohini R, Bose S. Tailoring the dispersion of multiwall carbon nanotubes in co-continuous PVDF/ABS blends to design materials with enhanced electromagnetic interference shielding. J Mater Chem A. 2015;3(15):7974–85.

[13] Ramôa SDAS, Barra, GMO, Oliveira RVB, de Oliveira MG, Cossa M, et al. Electrical, rheological and electromagnetic interference shielding properties of thermoplastic polyurethane/carbon nanotube composites. Polym Int. 2013;62(10):1477–84.

[14] Jean-Michel Thomassina IH, Jeromea R, Detrembleura C. Functionalized polypropylenes as efficient dispersing agents for carbon nanotubes in a polypropylene matrix; application to electromagnetic interference (EMI) absorber materials. Polymer. 2010;51:115–26.

[15] Pawar SP, Rzeczkowski P, Potschke P, Krause B, Bose S. Does the processing method resulting in different states of an interconnected network of multiwalled carbon nanotubes in polymeric blend nanocomposites affect EMI shielding properties? ACS Omega. 2018;3(5):5771–82.

[16] Ecco L, Dul S, Schmitz D, Barra G, Soares B, Fambri L, et al. Rapid prototyping of efficient electromagnetic interference shielding polymer composites via fused deposition modeling. Appl Sci. 2018;9(1):37–56.

[17] Dinesh P, Renukappa NM, Siddaramaiah, Sundara Rajan J. Electrical properties and EMI shielding characteristics of multiwalled carbon nanotubes filled carbon black-high density polyethylene nanocomposites. Composite Interfaces. 2012;19(2):121–33.

[18] Young SL, Yeon HP, Kwan HY. Flexural, electrical, thermal and electromagnetic interference shielding properties of xGnP and carbon nanotube filled epoxy hybrid nanocomposites. Carbon Lett. 2017;24:41–6.

[19] Sohi NJS, Rahaman M, Khastgir D. Dielectric property and electromagnetic interference shielding effectiveness of ethylene vinyl acetate-based conductive composites: effect of different type of carbon fillers. Polym Compos. 2011;32(7):1148–54.
[20] Jyoti J, Basu S, Singh BP, Dhakate SR. Superior mechanical and electrical properties of multiwall carbon nanotube reinforced acrylonitrile butadiene styrene high performance composites. Composites Part B. 2015;83:58–65.
[21] Shajari S, Arjmand M, Pawar SP, Sundararaj U, Sudak LJ. Synergistic effect of hybrid stainless steel fiber and carbon nanotube on mechanical properties and electromagnetic interference shielding of polypropylene nanocomposites. Composites Part B. 2019;165:662–70.
[22] Kumar GS, Vishnupriya D, Joshi A, Datar S, Patro TU. Electromagnetic interference shielding in 1–18 GHz frequency and electrical property correlations in poly(vinylidene fluoride)-multi-walled carbon nanotube composites. Phys Chem Chem Phys. 2015;17(31):20347–60.
[23] Al-Saleh MH. Electrical, EMI shielding and tensile properties of PP/PE blends filled with GNP:CNT hybrid nanofiller. Synth Met. 2016;217:322–30.
[24] Han MS, Lee YK, Lee HS, Yun CH, Kim WN. Electrical, morphological and rheological properties of carbon nanotube composites with polyethylene and poly(phenylene sulfide) by melt mixing. Chem Eng Sci. 2009;64(22):4649–56.
[25] Soares da Silva JP, Soares BG, Livi S, Barra GMO. Phosphonium-based ionic liquid as dispersing agent for MWCNT in melt-mixing polystyrene blends: rheology, electrical properties and EMI shielding effectiveness. Mater Chem Phys. 2017;189:162–8.
[26] Bagotia N, Choudhary V, Sharma DK. Synergistic effect of graphene/multiwalled carbon nanotube hybrid fillers on mechanical, electrical and EMI shielding properties of polycarbonate/ethylene methyl acrylate nanocomposites. Composites Part B. 2019;159:378–88.
[27] Al-Saleh MH, Sundararaj U. Microstructure, electrical, and electromagnetic interference shielding properties of carbon nanotube/acrylonitrile-butadiene-styrene nanocomposites. J Polym Sci Part B Polym Phys. 2012;50(19):1356–62.
[28] Basuli U, Chattopadhyay S, Nah C, Rout T. Electrical properties and electromagnetic interference shielding effectiveness of multiwalled carbon nanotubes-reinforced EMA nanocomposites. Polym Compos. 2012;33:897–903.
[29] Thomassin JM, Vuluga D, Alexandre M, Jérôme C, Molenberg I, Huynen I, et al. A convenient route for the dispersion of carbon nanotubes in polymers: application to the preparation of electromagnetic interference (EMI) absorbers. Polymer. 2012;53(1):169–74.
[30] Kum CK, Sung YT, Han MS, Kim WN, Lee HS, Lee SJ, et al. Effects of morphology on the electrical and mechanical properties of the polycarbonate/multi-walled carbon nanotube composites. Macromol Res. 2006;14(4):456–60.
[31] Mahmoodi M, Arjmand M, Sundararaj U, Park S. The electrical conductivity and electromagnetic interference shielding of injection molded multi-walled carbon nanotube/polystyrene composites. Carbon. 2012;50(4):1455–64.
[32] Gupta A, Choudhary V. Electrical conductivity and shielding effectiveness of poly(trimethylene terephthalate)/multiwalled carbon nanotube composites. J Mater Sci. 2011;46(19):6416–23.
[33] Das NC, Maiti S. Electromagnetic interference shielding of carbon nanotube/ethylene vinyl acetate composites. J Mater Sci. 2008;43(6):1920–5.
[34] Li QF, Xu Y, Yoon JS, Chen GX. Dispersions of carbon nanotubes/polyhedral oligomeric silsesquioxanes hybrids in polymer: the mechanical, electrical and EMI shielding properties. J Mater Sci. 2010;46(7):2324–30.
[35] Seyedi Ghezghapan SM, Javadi A. Effect of processing methods on electrical percolation and electromagnetic shielding of PC/MWCNTs nanocomposites. Polym Compos. 2017;269–76.
[36] Maiti S, Khatua BB. Graphene nanoplate and multiwall carbon nanotube-embedded polycarbonate hybrid composites: high electromagnetic interference shielding with low percolation threshold. Polym Compos. 2016;37(7):2058–69.
[37] Zhi X, Zhang HB, Liao YF, Hu QH, Gui CX, Yu ZZ. Electrically conductive polycarbonate/carbon nanotube composites toughened with micron-scale voids. Carbon. 2015;82:195–204.
[38] Mathur RB, Pande S, Singh BP, Dhami TL. Electrical and mechanical properties of multi-walled carbon nanotubes reinforced PMMA and PS composites. Polym Compos. 2008;29(7):717–27.
[39] Jin X, Ni QQ, Natsuki T. Composites of multi-walled carbon nanotubes and shape memory polyurethane for electromagnetic interference shielding. J Compos Mater. 2011;45(24):2547–54.
[40] Tan YJ, Li J, Cai JH, Tang XH, Liu JH, Hu ZQ, et al. Comparative study on solid and hollow glass microspheres for enhanced electromagnetic interference shielding in polydimethylsiloxane/multi-walled carbon nanotube composites. Composites Part B. 2019;177:107378–88.
[41] Singh BP, Prasanta V, Choudhary V, Saini P, Pande S, Singh VN, et al. Enhanced microwave shielding and mechanical properties of high loading MWCNT–epoxy composites. J Nanopart Res. 2013;15(4):1–12.
[42] Liu Y, Song D, Wu C, Leng J. EMI shielding performance of nanocomposites with MWCNTs, nanosized Fe_3O_4 and Fe. Composites Part B. 2014;63:34–40.
[43] Mittal G, Rhee KY, Park SJ. The effects of cryomilling CNTs on the thermal and electrical properties of CNT/PMMA composites. Polymers. 2016;8(5):169–82.
[44] Pande S, Chaudhary A, Patel D, Singh BP, Mathur RB. Mechanical and electrical properties of multiwall carbon nanotube/polycarbonate composites for electrostatic discharge and electromagnetic interference shielding applications. RSC Adv. 2014;4(27):13839–49.
[45] Kuzhir P, Paddubskaya A, Bychanok D, Nemilentsau A, Shuba M, Plusch A, et al. Microwave probing of nanocarbon based epoxy resin composite films: toward electromagnetic shielding. Thin Solid Films. 2011;519:4114–8.
[46] Eswaraiah V, Sankaranarayanan V, Ramaprabhu S. Inorganic nanotubes reinforced polyvinylidene fluoride composites as low-cost electromagnetic interference shielding materials. Nanoscale Res Lett. 2011;6(1):137–48.
[47] Rath SK, Dubey S, Kumar GS, Kumar S, Patra AK, Bahadur J, et al. Multi-walled CNT-induced phase behaviour of poly

(vinylidene fluoride) and its electro-mechanical properties. J Mater Sci. 2013;49(1):103–13.
[48] Al-Saleh MH, Saadeh WH, Sundararaj U. EMI shielding effectiveness of carbon based nanostructured polymeric materials: a comparative study. Carbon. 2013;60:146–56.
[49] Saini P, Choudhary V. Enhanced electromagnetic interference shielding effectiveness of polyaniline functionalized carbon nanotubes filled polystyrene composites. J Nanopart Res. 2013;15(1):1415–22.
[50] Lin JH, Lin ZI, Pan YJ, Hsieh CT, Huang CL, Lou CW. Thermoplastic polyvinyl alcohol/multiwalled carbon nanotube composites: preparation, mechanical properties, thermal properties, and electromagnetic shielding effectiveness. J Appl Polym Sci. 2016;133:43474–84.
[51] Zhang H, Zhang G, Tang M, Zhou L, Li J, Fan X, et al. Synergistic effect of carbon nanotube and graphene nanoplates on the mechanical, electrical and electromagnetic interference shielding properties of polymer composites and polymer composite foams. Chem Eng J. 2018;353:381–93.
[52] Kim MS, Yan J, Joo KH, Pandey JK, Kang YJ, Ahn SH. Synergistic effects of carbon nanotubes and exfoliated graphite nanoplatelets for electromagnetic interference shielding and soundproofing. J Appl Polym Sci. 2013;130:3947–51.
[53] Bagotia N, Mohite H, Tanaliya N, Sharma DK. A comparative study of electrical, EMI shielding and thermal properties of graphene and multiwalled carbon nanotube filled polystyrene nanocomposites. Polym Compos. 2018;39(2):1041–51.
[54] Wang XH, Mu YH, Tang Q, Li CQ. Preparation and performance of PVC/CNT nanocomposite. Adv Polym Technol. 2018;37(2):358–64.
[55] Hayashida K, Matsuoka Y. Electromagnetic interference shielding properties of polymer-grafted carbon nanotube composites with high electrical resistance. Carbon. 2015;85:363–71.
[56] Park SH, Paul TT, Peter MA, Prabhakar RB. Enhanced electromagnetic interference shielding through the use of functionalized carbon-nanotube-reactive polymer composites. IEEE Trans Nanotechnol. 2010;9(4):464–9.
[57] Mohanty AK, Ghosh A, Sawai P, Pareek K, Banerjee S, Das A, et al. Electromagnetic interference shielding effectiveness of MWCNT filled poly(ether sulfone) and poly(ether imide) nanocomposites. Polym Eng Sci. 2014;54(11):2560–70.
[58] Sun X, Liu X, Shen X, Wu Y, Wang Z, Kim JK. Graphene foam/carbon nanotube/poly(dimethyl siloxane) composites for exceptional microwave shielding. Composites Part A. 2016;85:199–206.
[59] Ren F, Li Z, Xu L, Sun Z, Ren P, Yan D, et al. Large-scale preparation of segregated PLA/carbon nanotube composite with high efficient electromagnetic interference shielding and favourable mechanical properties. Composites Part B. 2018;155:405–13.
[60] Al-Saleh MH. Influence of conductive network structure on the EMI shielding and electrical percolation of carbon nanotube/polymer nanocomposites. Synth Met. 2015;205:78–84.
[61] Chen Y, Zhang HB, Yang Y, Wang M, Cao A, Yu ZZ. High-performance epoxy nanocomposites reinforced with three-dimensional carbon nanotube sponge for electromagnetic interference shielding. Adv Funct Mater. 2016;26(3):447–55.
[62] Cui CH, Yan DX, Pang H, Jia LC, Xu X, Yang S, et al. A high heat-resistance bioplastic foam with efficient electromagnetic interference shielding. Chem Eng J. 2017;323:29–36.
[63] Ursache Ş, Ciobanu RC, Scarlatache V, Niagu A. Dielectric and electromagnetic behavior of conductive nanocomposites polymers: PP/MWCNT investigations for EMI applications. Adv Eng Forum. 2013;8(9):353–60.
[64] Hoang AS. Electrical conductivity and electromagnetic interference shielding characteristics of multiwalled carbon nanotube filled polyurethane composite films. Adv Nat Sci Nanosci Nanotechnol. 2011;2(2):1–6.
[65] Gupta TK, Singh BP, Dhakate SR, Singh VN, Mathur RB. Improved nanoindentation and microwave shielding properties of modified MWCNT reinforced polyurethane composites. J Mater Chem A. 2013;1(32):9138–65.
[66] Liu Z, Bai G, Huang Y, Li F, Ma Y, Guo T, et al. Microwave absorption of single-walled carbon nanotubes/soluble cross-linked polyurethane composites. J Phys Chem. 2007;111:13696–700.
[67] Gupta TK, Singh BP, Teotia S, Katyal V, Dhakate SR, Mathur RB. Designing of multiwalled carbon nanotubes reinforced polyurethane composites as electromagnetic interference shielding materials. J Polym Res. 2013;20(6):169–76.
[68] Farukh M, Dhawan R, Singh BP, Dhawan SK. Sandwich composites of polyurethane reinforced with poly(3,4-ethylene dioxythiophene)-coated multiwalled carbon nanotubes with exceptional electromagnetic interference shielding properties. RSC Adv. 2015;5(92):75229–38.
[69] Kim HM, Kim K, Lee CY, Joo J, Cho SJ, Yoon HS, et al. Electrical conductivity and electromagnetic interference shielding of multiwalled carbon nanotube composites containing Fe catalyst. Appl Phys Lett. 2004;84(4):589–91.
[70] Kim HM, Kim K, Lee SJ, Joo J, Yoon HS, Cho SJ, et al. Charge transport properties of composites of multiwalled carbon nanotube with metal catalyst and polymer: application to electromagnetic interference shielding. Curr Appl Phys. 2004;4(6):577–80.
[71] Li N, Huang Y, Du F, He X, Lin X, Gao H, et al. Electromagnetic interference (EMI) shielding of single-walled carbon nanotube epoxy composites. Am Chem Soc. 2006;6:1141–5.
[72] Singh AP, Gupta BK, Mishra M, Govind, Chandra A, Mathur RB, et al. Multiwalled carbon nanotube/cement composites with exceptional electromagnetic interference shielding properties. Carbon. 2013;56:86–96.
[73] Gupta A, Choudhary V. Electromagnetic interference shielding behavior of poly(trimethylene terephthalate)/multi-walled carbon nanotube composites. Compos Sci Technol. 2011;71(13):1563–8.
[74] Farukh M, Singh AP, Dhawan SK. Enhanced electromagnetic shielding behavior of multi-walled carbon nanotube entrenched poly(3,4-ethylenedioxythiophene) nanocomposites. Compos Sci Technol. 2015;114:94–102.
[75] Thomassin JM, Pagnoulle C, Bednarz L, Huynen I, Jerome R, Detrembleur C. Foams of polycaprolactone/MWNT nanocomposites for efficient EMI reduction. J Mater Chem. 2008;18(7):792–7.

[76] Al-Saleh MH, Sundararaj U. Electromagnetic interference shielding mechanisms of CNT/polymer composites. Carbon. 2009;47(7):1738–46.
[77] Yang Y, Mool CG, Kenneth LD, Roland WL. Novel carbon nanotube-polystyrene foam composites for electromagnetic interference shielding. Am Chem Soc. 2005;5:2131–4.
[78] Huang CY, Wu JY, Tsao KY, Lin CL, Chang CP, Tsai CS, et al. The manufacture and investigation of multi-walled carbon nanotube/polypyrrole/EVA nano-polymeric composites for electromagnetic interference shielding. Thin Solid Films. 2011;519(15):4765–73.
[79] Huang Y, Li N, Ma Y, Du F, Li F, He X, et al. The influence of single-walled carbon nanotube structure on the electromagnetic interference shielding efficiency of its epoxy composites. Carbon. 2007;45(8):1614–21.
[80] Hornbostel B, Leute U, Pötschke P, Kotz J, Kornfeld D, Chiu PW, et al. Attenuation of electromagnetic waves by carbon nanotube composites. Phys E. 2008;40(7):2425–9.
[81] Park SH, Ha JH. Improved electromagnetic interference shielding properties through the use of segregate carbon nanotube networks. Materials. 2019;12(9):1395–403.
[82] Arjmand M, Sadeghi S, Otero Navas I, Zamani Keteklahijani Y, Dordanihaghighi S, Sundararaj U. Carbon nanotube versus graphene nanoribbon: impact of nanofiller geometry on electromagnetic interference shielding of polyvinylidene fluoride nanocomposites. Polymers. 2019;11(6):1064–78.
[83] Arjmand M, Sundararaj U. Electromagnetic interference shielding of nitrogen-doped and undoped carbon nanotube/polyvinylidene fluoride nanocomposites: a comparative study. Compos Sci Technol. 2015;118:257–63.
[84] Li Y, Chen C, Zhang S, Ni Y, Huang J. Electrical conductivity and electromagnetic interference shielding characteristics of multiwalled carbon nanotube filled polyacrylate composite films. Appl Surf Sci. 2008;254(18):5766–71.
[85] Nam IW, Lee HK, Jang JH. Electromagnetic interference shielding/absorbing characteristics of CNT-embedded epoxy composites. Composites Part A. 2011;42(9):1110–8.
[86] Kong L, Yin X, Yuan X, Zhang Y, Liu X, Cheng L, et al. Electromagnetic wave absorption properties of graphene modified with carbon nanotube/poly(dimethyl siloxane) composites. Carbon. 2014;73:185–93.
[87] Pande S, Singh B, Mathur R, Dhami T, Saini P, Dhawan S. Improved electromagnetic interference shielding properties of MWCNT-PMMA composites using layered structures. Nanoscale Res Lett. 2009;4(4):327–34.
[88] Silva V, Rezende MC. Effect of the morphology and structure on the microwave absorbing properties of multiwalled carbon nanotube filled epoxy resin nanocomposites. Mater Res. 2018;21(5):1–9.
[89] Phan CH, Mariatti M, Koh YH. Electromagnetic interference shielding performance of epoxy composites filled with multiwalled carbon nanotubes/manganese zinc ferrite hybrid fillers. J Magnet Magnet Mater. 2016;401:472–8.
[90] Hoang AS, Nguyen HN, Bui HT, Tran AT, Duong VA, Nguyen VB. Carbon nanotubes materials and their application to guarantee safety from exposure to electromagnetic fields. Adv Nat Sci Nanosci Nanotechnol. 2013;4(2):025012–8.
[91] Bal S, Saha S. Scheming of microwave shielding effectiveness for X band considering functionalized MWNTs/epoxy composites. IOP Conf Ser Mater Sci Eng. 2016;115:012027–37.
[92] Micheli D, Apollo C, Pastore R, Marchetti M. X-Band microwave characterization of carbon-based nanocomposite material, absorption capability comparison and RAS design simulation. Compos Sci Technol. 2010;70(2):400–9.
[93] Singh BP, Veena C, Parveen S, Mathur RB. Designing of epoxy composites reinforced with carbon nanotubes grown carbon fiber fabric for improved electromagnetic interference shielding. J Appl Phys. 2011;2:022151–6.
[94] Duan H, Zhu H, Yang J, Gao J, Yang Y, Xu L, et al. Effect of carbon nanofiller dimension on synergistic EMI shielding network of epoxy/metal conductive foams. Composites Part A. 2019;118:41–8.
[95] Kunjappan AM, Poothanari MA, Ramachandran AA, Padmanabhan M, Mathew L, Thomas S. High-performance electromagnetic interference shielding material based on an effective mixing protocol. Polym Int. 2019;68(4):637–47.
[96] Yuan B, Yu L, Sheng L, An K, Zhao X. Comparison of electromagnetic interference shielding properties between single-wall carbon nanotube and graphene sheet/polyaniline composites. J Phys D Appl Phys. 2012;45(23):1–8.
[97] Yuen SM, Ma CCM, Chuang CY, Yu KC, Wu SY, Yang CC, et al. Effect of processing method on the shielding effectiveness of electromagnetic interference of MWCNT/PMMA composites. Compos Sci Technol. 2008;68(3):963–8.
[98] Jia LC, Yan DX, Yang Y, Zhou D, Cui CH, Bianco E, et al. High strain tolerant EMI shielding using carbon nanotube network stabilized rubber composite. Adv Mater Technol. 2017;2(7):1–6.
[99] Jia LC, Yan DX, Cui CH, Ji X, Li ZM. A unique double percolated polymer composite for highly efficient electromagnetic interference shielding. Macromol Mater Eng. 2016;301(10):1232–41.
[100] Lu D, Mo Z, Liang B, Yang L, He Z, Zhu H, et al. Flexible, lightweight carbon nanotube sponges and composites for high-performance electromagnetic interference shielding. Carbon. 2018;133:457–63.
[101] Xu Y, Li Y, Hua W, Zhang A, Bao J. Light-weight silver plating foam and carbon nanotube hybridized epoxy composite foams with exceptional conductivity and electromagnetic shielding property. ACS Appl Mater Interfaces. 2016;8(36):24131–42.
[102] Kuang T, Chang L, Chen F, Sheng Y, Fu D, Peng X. Facile preparation of lightweight high-strength biodegradable polymer/multi-walled carbon nanotubes nanocomposite foams for electromagnetic interference shielding. Carbon. 2016;105:305–13.
[103] Yang Y, Gupta MC, Dudley KL, Lawrence RW. Novel carbon nanotube–polystyrene foam composites for electromagnetic interference shielding. Nano Lett. 2005;5(11):2131–4.
[104] Zhang H, Zhang G, Li J, Fan X, Jing Z, Li J, et al. Lightweight, multifunctional microcellular PMMA/Fe_3O_4@MWCNTs nanocomposite foams with efficient electromagnetic interference shielding. Composites Part A. 2017;100:128–38.
[105] Xu L, Jia LC, Yan DX, Ren PG, Xu JZ, Li ZM. Efficient electromagnetic interference shielding of lightweight carbon

nanotube/polyethylene composites via compression molding plus salt-leaching. RSC Adv. 2018;8(16):8849–55.
[106] Sambyal P, Iqbal A, Hong J, Kim H, Kim MK, Hong SM, et al. Ultralight and mechanically robust $Ti_3C_2T_x$ hybrid aerogel reinforced by carbon nanotubes for electromagnetic interference shielding. ACS Appl Mater Interfaces. 2019;11(41):38046–54.
[107] Thomassin JM, Jérôme R, Detrembleur C, Molenberg I, Huynen I. Polymer/carbon nanotube composites for electromagnetic interference reduction. Materials Science and Engineering: R: Reports. 2010;74:563–87.
[108] Thomassin JM, Lou X, Pagnoulle C, Saib A, Bednarz L, Huynen I, et al. Multiwalled carbon nanotube/poly(ε-caprolactone) nanocomposites with exceptional electromagnetic interference shielding properties. J Phys Chem C. 2007;111(30):11186–92.
[109] Huang YL, Yuen SM, Ma CCM, Chuang CY, Yu KC, Teng CC, et al. Morphological, electrical, electromagnetic interference (EMI) shielding, and tribological properties of functionalized multi-walled carbon nanotube/poly methyl methacrylate (PMMA) composites. Compos Sci Technol. 2009;69(11–12):1991–6.
[110] Hirako K, Shirasaka S, Obata T, Nakasuka S, Saito H, Nakamura S, et al. Development of small satellite for X-Band compact synthetic aperture radar. J Phys Conf Ser. 2018;1130:012013–23.
[111] Shrestha S, Choi DY. Rain attenuation study at Ku-band over earth–space path in South Korea. Adv Astron. 2019;2019:1–12.
[112] Takizawa K, Hashimoto O. Transparent wave absorber using resistive thin film at V-band frequency. IEEE Trans Microw Theory Tech. 1999;47(7):1137–41.
[113] Hasan M, Bianchi C. Ka band enabling technologies for high throughput satellite (HTS) communications. Int J Satell Commun Netw. 2016;34(4):483–501.
[114] Moldovan IA, Biagi PF, Moldovan AS, Placinta AO. The infrep European VLF/LF radio monitoring. Netw Present Status Preliminary Results Romanian Monit Syst. 2010;64:263–74.
[115] Hazmin Sabri N, Nurul Aisyah Syed Zafar S, Umar R, Mat R. Northeast monsoon effect on ultra high frequency (UHF) signal attenuation at Kusza observatory. J Phys Conf Ser. 2019;1152:012009–18.
[116] Rajabi H, Aksoy M. Characteristics of the L-band radio frequency interference environment based on SMAP radiometer observations. IEEE Geosci Remote Sens Lett. 2019;16(11):1–5.
[117] Samsuzzaman M, Islam MT, Arshad H, Mandeep JS, Misran N. Circularly polarized S band dual frequency square patch antenna using glass microfiber reinforced PTFE composite. Sci World J. 2014;2014:345190–200.
[118] Monti-Guarnieri A, Giudici D, Recchia A. Identification of C-band radio frequency interferences from sentinel-1 data. Remote Sens. 2017;9(11):1183–95.
[119] Rahman S, Robertson DA. Radar micro-doppler signatures of drones and birds at K-band and W-band. Sci Rep. 2018;8(1):17396–407.
[120] Hamed A, Habibpour O, Saeed M, Zirath H, Negra R. W-band graphene-based six-port receiver. IEEE Microw Wirel Compon Lett. 2018;28(4):347–9.
[121] Kumar M, Ando Y. Chemical vapor deposition of carbon nanotubes: a review on growth mechanism and mass production. J Nanosci Nanotechnol. 2010;10(6):3739–58.
[122] Mamunya Y, Matzui L, Vovchenko L, Maruzhenko O, Oliynyk V, Pusz S, et al. Influence of conductive nano- and microfiller distribution on electrical conductivity and EMI shielding properties of polymer/carbon composites. Compos Sci Technol. 2019;170:51–9.
[123] Xie Z, Zhuang Q, Wang Q, Liu X, Chen Y, Han Z. *In situ* synthesis and characterization of poly(2,5-benzoxazole)/multiwalled carbon nanotubes composites. Polymer. 2011;52(23):5271–6.
[124] Park C, Ounaies Z, Watson KA, Crooks RE, Smith J, Lowther SE, et al. Dispersion of single wall carbon nanotubes by *in situ* polymerization under sonication. Chem Phys Lett. 2002;364(3):303–8.
[125] Zhang CS, Ni QQ, Fu SY, Kurashiki K. Electromagnetic interference shielding effect of nanocomposites with carbon nanotube and shape memory polymer. Compos Sci Technol. 2007;67(14):2973–80.
[126] Wu HY, Jia LC, Yan DX, Gao JF, Zhang XP, Ren PG, et al. Simultaneously improved electromagnetic interference shielding and mechanical performance of segregated carbon nanotube/polypropylene composite via solid phase molding. Compos Sci Technol. 2018;156:87–94.
[127] Jia LC, Yan DX, Jiang X, Pang H, Gao JF, Ren PG, et al. Synergistic effect of graphite and carbon nanotubes on improved electromagnetic interference shielding performance in segregated composites. Ind Eng Chem Res. 2018;57(35):11929–38.
[128] Pang H, Xu L, Yan DX, Li ZM. Conductive polymer composites with segregated structures. Prog Polym Sci. 2014;39(11):1908–33.
[129] Wang H, Zheng K, Zhang X, Du T, Xiao C, Ding X, et al. Segregated poly(vinylidene fluoride)/MWCNTs composites for high-performance electromagnetic interference shielding. Composites Part A. 2016;90:606–13.
[130] Zhang K, Li GH, Feng LM, Wang N, Guo J, Sun K, et al. Ultralow percolation threshold and enhanced electromagnetic interference shielding in poly(L-lactide)/multi-walled carbon nanotube nanocomposites with electrically conductive segregated networks. J Mater Chem C. 2017;5(36):9359–69.
[131] Raagulan K, Braveenth R, Kim BM, Lim KJ, Lee SB, Kim M, et al. An effective utilization of MXene and its effect on electromagnetic interference shielding: flexible, free-standing and thermally conductive composite from MXene–PAT–poly(*p*-aminophenol)–polyaniline co-polymer. RSC Adv. 2020;10(3):1613–33.
[132] Yuen SM, Ma CCM, Chuang CY, Yu KC, Wu SY, Yang CC, et al. Effect of processing method on the shielding effectiveness of electromagnetic interference of MWCNT/PMMA composites. Compos Sci Technol. 2008;68(3–4):963–8.
[133] Li J, Zhang G, Zhang H, Fan X, Zhou L, Shang Z, et al. Electrical conductivity and electromagnetic interference shielding of epoxy nanocomposite foams containing functionalized multi-wall carbon nanotubes. Appl Surf Sci. 2018;428:7–16.
[134] Huynen I, Quiévy N, Bailly C, Bollen P, Detrembleur C, Eggermont S, et al. Multifunctional hybrids for electromagnetic absorption. Acta Mater. 2011;59(8):3255–66.